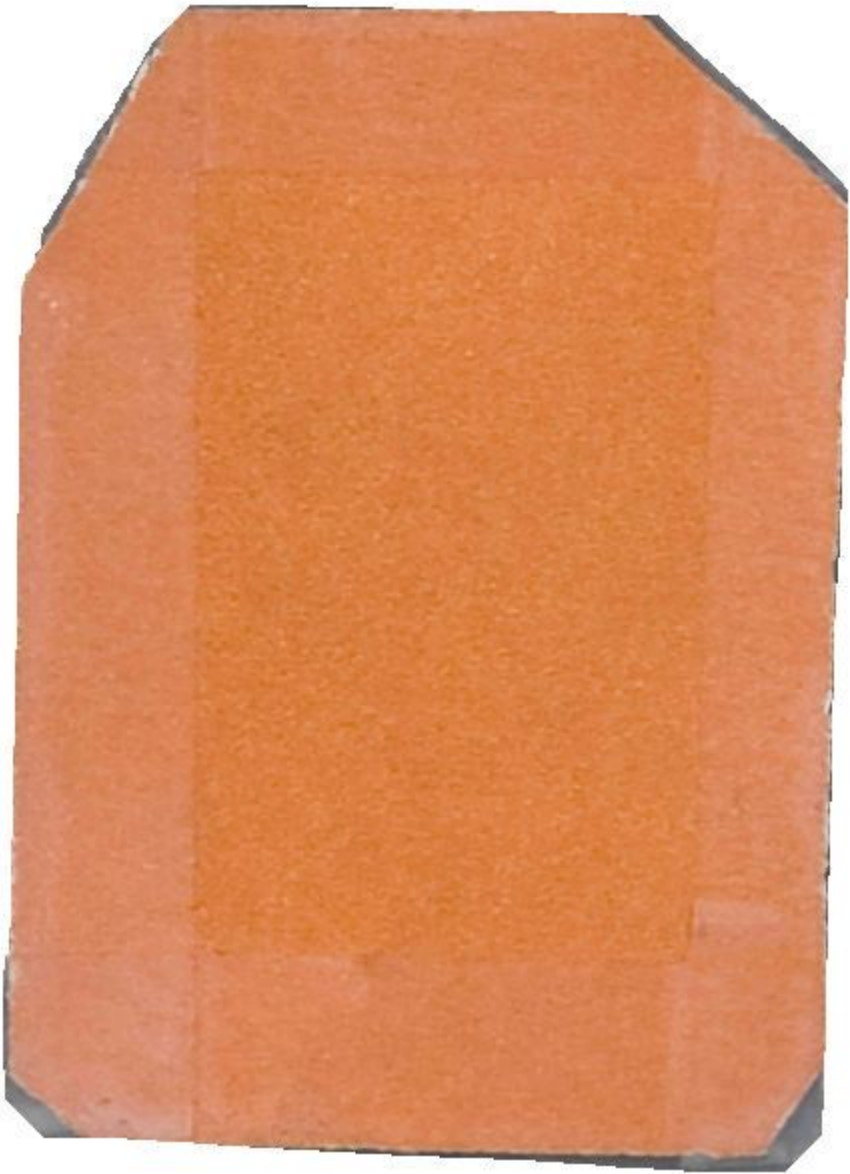

SPS

Rapport des étudiants 64a

(1619)

95001 t/m 95043

GENESIS OF IRON CRUSTS IN BURKINA FASO

L. de Boer
June 1995

Aménagement et Gestion
de l'Espace Sylvo-Pastoral au Sahel

Antenne Sahélienne de l'Université Agronomique Wageningen Pays-Bas
et de l'Université de Ouagadougou Burkina Faso

PUBLICATIONS DEJA PARUES:

Documents du projet (rouge)

1	B. van Koppen & N. Groesz	Research Proposal: "gender in the optimalization of tenure arrangements with regard to landesque capital"
2	J. Oostveen (red.)	Werkplannen juni 1991
3	B. Lekanne dit Deprez	Silvopastorale gebieden als sociale ruimte bij de Mossi van Burkina Faso
4	E. Frederiks	Algemene informatie ten behoeve van bezoek aan de Universiteit van Ouagagdougou
5	E. Frederiks	Programme Sahélien UAW: Activités 1985 - 1992 et l'avenir
6	M. Bloemberg (red.)	Rapport du 1er atelier du programme de recherche SPS à Ouagadougou (du 14 au 18 décembre 1992
7	A. de Wit	Manuel pour mésurer la sève des arbres avec le "Dynamax sap flow system flow32"
8	L. Stroosnijder & W. Hoogmoed	Zelfevaluatie VF-Sahel (VF 91.61), februari 1993
9	A. Ran	Hoe, wat, waar in Burkina Faso: studentenhandleiding Steunpunt Sahel
10	M. Rietkerk & F. Hien	Mesures de régénération au Sahel
11	A. Mando	Role des termites dans la régénération des sols dégradés au Sahel
12	L. Stroosnijder & W. Hoogmoed	"Management of natural resources in the sahel", subprogramme of the VF-programme "Sustainable land use in the tropics"
13	M.A. Mulders	Rapport sur les activités de télédetection du programme SPS, juillet 1992 - mai 1993
14	M.A. Mulders, J. van Rooijen et A. Casterad	Data processing as preparation for soil and land degradation studies in Burkina Faso
15	A. Bleumink	Manuel pour l'utilisation de l'enregistreur de données DELTA-T logger
16	E. Frederiks (red.)	Rapport Annuel 1992, Antenne Sahéliene UO/UAW (version française et néerlandaise)
17	H.J.F. Savenije	Sylvicultural management practices in the Sudan and Sahel zone with an emphasis on the silvopastoral vegetations: a compilation of literature
18	J.W. Nibbering	Manuel de quelques techniques de mesures agro-économiques et le traitement des résultats
19		Rapport Annuel 1993, Antenne Sahéliene UO/UAW, mars 1994
20	J.W. Nibbering	Méthode et résultats de quelques transects effectués le long des routes de circulation pour inventorier l'état et l'utilisation des terroirs au niveau régional
21	J.W. Nibbering	Glossaires français-néerlandais et néerlandais-français de termes utilesés dans l'étude des aspects sociaux et économiques de l'agriculture
23	J.W. Nibbering	Liste des termes français-neérlandais et néerlandais-français employés pour la description de l'état des paysages, des processus s'y déroulant et des agents modificateurs
24	J. Begemann e.a.	Antenne Sahélienne UAW/UO. Rapport Annuel 1994 et Perspectives 1995
27	J.W. Nibbering	Modelling of resource utilization and management: Models presented at the PSS/DLV/ESPGRN-Sikasso workshop in Niono from 18 to 20 september 1994
28	J. de Graaff	La situation agro-economiques et les mesures anti-erosives dans six villages sur le plateau mossi (Quelques données des enquêtes agro-économiques 1992-1994)

Publications de l'Antenne (vert)

1	S. de Bie & C. Geerling	IUCN-Paper: "Ecological Limits to the conservation and sustainable exploitation of natural resources"
2	W. van Driel & A. Ran	Risques et contraintes pour l'intensification de la riziculture dans deux bas-fonds aménages de la province de la Comoë, Burkina Faso
3	J.J. Kessler & K.F. Wiersum	The multi-dimensional nature of silvo-pastoral areas in the Sahel region
4	L. Stroosnijder	Afrika studiedag 16 december 1992: "Ecologisch kwetsbare gebieden in Afrika"
5	L. Stroosnijder, W. B. Hoogmoed and J.J.A. Berkhout	Séminaire International sur la gestion agroclimatique des precipitations, décembre 1991: "Modelling effects of water conservation tillage in the semi-arid tropics"
6	W.B. Hoogmoed J.J.A. Berkhout L. Stroosnijder	Séminaire Internationale sur le travail du sol en zones arides et semi-arides, organisé par l'ANAFID, 22-23 april 1992: "Soil tillage options for water management under erratic rainfall conditions"
7	M. Rietkerk, F. Hien L. Stroosnijder	"Dominance des caractères des croûtes sur les types de sols dans les terrains sylvo-pastoraux dégradés au Sahel"
8	J.J. Kessler	Agroforestry and Sustainable Land-use in Semi-arid Africa. In: Zeitschrift für Wirtschaftsgeographie, Jg. 37 (1993), Heft 2, S. 68-77, Frankfurt a.M.
9	J.J. Kessler & K.F. Wiersum	Ecological Sustainability of Agroforestry in the Tropics. In: Entwicklung und Ländlicher Raum 5/93, vol 27 (5): 8 - 11, 1993
10	K.F. Wiersum	Systèmes indigènes d'exploitation et de gestion de la végétation boisée au Sénégal: cadre d'analyse. In: La Foresterie Rurale au Sénégal: participation villageoise et gestion locale, Leiden Development Studies, No. 12: 135 - 159, 1993
11	L. Stroosnijder	Population Density, Carrying Capacity and Agricultural Production Technology in the Sahel. Paper presented at the 1994 Danish Sahel Workshop, 6-8 January 1994, Sandberg Manor, Sonderborg, Denmark
12	A. Mando, W.F. van Driel & N. Prosper Zombré	Le rôle des termites dans la restauration des sols ferrugineux tropicaux encroûtés au Sahel. Contribution au 1er Colloque International de l'AOCASS: Gestion Durable des Sols et de l'Environnement en Afrique Tropicale, Ouagadougou, 6 - 10 décembre 1994

GENESIS OF IRON CRUSTS IN BURKINA FASO

Agricultural University
Wageningen

Wageningen, June 1995

Under authority of:
ir D. Legger

Linda de Boer
71-06-23-083-040

PREFACE

This report was made in connection with my study at the Agricultural University in Wageningen. The aim of this report is to unravel the process of the genesis of iron crusts in Burkina Faso, West Africa.

First I'd like to thank Piet van Asten, Douwe Dijkstra, Gisbert van Ginkel, Jacqueline van der Pol, Marcel Steenis and Dirk Wijnalda. They joined me during my stay in Burkina Faso and helped me making this journey successfull.

Furthermore I wish to acknowledge the support of Maarten Tromp. He was of great help discussing field observations and determining sampling sites.

I'm particularly indebted to the staff of Antenne Sahélienne for their support in arranging housing and transport.

I'd like to thank Jan van Doesburg and Bram Kuiper for performing X-ray diffraction and rontgen fluorescency analysis.

My appreceation goes also to Toine Jongmans for his help in making thin sections descriptions and interpertations.

Finally I wish to acknowledge the support of Dick Legger both during my stay in Burkina Faso and afterwards when making the report.

Wageningen, June 1995
Linda de Boer

CONTENT

SUMMARY

Iron crusts (hardened plinthite or laterites) are commonly found in Burkina Faso. In the research area three levels of iron crusts are found. Furthermore granodiorite is found at the soil surface. The granodiorite is thought to be the parent material, because areas of slightly weathered granodiorite were found in the subsoil of the middle iron crust. Micromorphological observations confirm that the material at the three levels of iron crusts is derived from the granodiorite.

At the middle iron crust the profile consists of white sandy loam to sandy clay loam with yellow and red to yellowish red mottles. With decreasing depth the area covered by mottles increases, by an increase in their size, suggesting growth of mottles. Locally the red or the yellow mottles are dominant. In the upper part of the profile reddish brown iron nodules are found. The top of the profile consists of an iron crust. The iron crust is red, reddish yellow and black and has hardened on exposure. Field observations make clear that the iron crust consists of two clearly separated layers. The lower part seems to have formed in situ whereas the upper part consists of cemented iron gravel.

Micromorphologically the granodiorite consists of quartz minerals, alkali feldspars, green hornblendes, biotite and opaque iron minerals. Iron-bearing minerals like hornblendes, biotite and opaque iron minerals are found in a clustered distribution pattern.
Micromorphological observations of the samples of the middle iron crust suggest that, upon weathering of the granodiorite, a yellow saprolite is formed, consisting of clay booklets and angular quartz grains. When the granodiorite weathers the alkali feldspars are transformed into clay booklets, probably kaolinite. Mineralogical analysis confirm the presence of much kaolinite in all samples except for the granodiorite and for slightly weathered granodiorite.
Due to periodically hydromorphic processes a white saprolite and orange red iron nodules are formed. The transition from iron nodules to white saprolite is diffuse, suggesting an in situ formation. Appreciable amounts of iron-bearing minerals are found in the iron nodules whereas such features occasionally occur in the white coloured saprolite. Iron-bearing minerals, which were found in a clustered distribution pattern in the parent material, seem to act as cores around which iron formation occurs. When hydromorphic processes proceed, when going up in the profile, the area covered by iron nodules increases and different areas grow together. Quartz minerals are locally enclosed by iron. Weathering of the quartz minerals results in the formation of rectangular voids. A framework of iron remains.
Field observations, suggesting a difference between the two layers of the middle iron crust, are confirmed by micromorphological analysis. A red clayey material found in the lower part of the iron crust is not found in the upper part. The red

material is thought to have covered the yellow saprolite. At the moment only pieces of the red material are present. No continous layer is found suggesting that the majority of the red B horizon has eroded. After erosion, the upper part of the iron crust must have formed. The upper part of the iron crust consists of spherical, sharply bounded iron concretions. Quartz or other primary minerals are hardly found present. The sharply bounded iron concretions are supposed to be detrital coming from adjacent areas.
In the profile locally clay coatings are found, which are occasionally covered by lime. The presence of lime can be the result of either termite activity or capillary rise.

Field observations suggested the highest elevated iron crust to consist of a similar profile as the middle iron crust. However, instead of white sandy loam (which was predominantly found at the middle iron crust), red sandy loam to clay was found. Micromorphological and field observations reveal that the highest elevated iron crust is more heavily impregnated with iron, which makes it hard to distinguish mottles. At the foot of the highest elevated iron crust micromorphological observations revealed the presence of a heterogeneous yellow-red soil material and dark red, sharply bounded iron gravel of alternating mineralogical composition and size. Both heterogenous fabric and sharp bounderies suggest it to be detrital coming from higher altitudes. The highest elevated iron crust is formed in situ. At lower altitudes however in situ material can be covered with detrital.

Field observations do not distinguish whether the lowest iron crust, which is rather thin, is formed in situ or is formed due to cementation of iron gravel from higher altitudes. Micromorphological observations revealed that both processes took place.

Field- and micromorphological observations, in combination with chemical analysis, revealed that six processes took place in iron crust formation in the following order:
Loss of Na_2O, K_2O, BaO, CaO, MnO and MgO, ferralitisation, ferrolysis, iron accumulation, clay illuviation and translocation of lime.

Graphical presentations of the four major elements SiO_2, TiO_2, Fe_2O_3 and Al_2O_3 can be used to determine the age of every iron crust in the area. These graphs reveal the absolute amounts of different elements in the profile. As different crusts occur at different locations in the graph, the relative age of each crust could be determined in this way.

Furthermore these figures reveal the absolute amounts of SiO_2, Al_2O_3 and Fe_2O_3 that leached from or accumulated in the profile. The extend of iron accumulation suggests that iron transport must partially and may totally originate from adjacent (topographically higher) areas. Laterites (iron crusts) may also have been formed as a precipitates (from underlying horizons) or as a residuum (from overlying horizons).

1 INTRODUCTION

In the eigthteenth century the existence of a rather soft and iron-rich building material was reported for the first time. The material was soft while excluded from air but hardened upon exposure to the atmosphere. In 1807 Buchanan started to use the term laterite (latericius L. = brick) for this material. In India he found laterite overlying granite. The granite was full of cavities and pores, and contained a very large quantity of iron in the form of red and yellow ochres.

At the moment the term laterite is commonly used for "highly weathered red subsoil or material, rich in secondary oxides of iron, aluminium, or both, nearly devoid of bases and primary silicates, and commonly with quartz and kaolinite..." (Bates and Jackson, 1980).

Laterite is of interest because of its importance as a source of economically important metals and because it is difficult to grow crops on.

Laterite is found in tropical areas with pronounced wet and dry periods. It is assumed that not the lithology but the micro environment determines laterite development, because in certain areas the presence of certain parent material stimulates the formation of laterite whereas in other areas the same parent material declines its formation (McFarlane, 1976). The micro environment is determined by a combination of factors such as climate, topography, lithology, porosity and grain size distribution. A relation with the lithology is often expressed by less clear accumulations than those of iron and aluminium e.g. accumulations of trace elements or heavy minerals.
Differences in parent material result into different types of laterite. A granodiorite parent material will result in a ferruginous laterite (Aleva, 1994).
The process of laterite formation is still not clear. Three theories have been developed to explain its development being:

1. Laterite as a residuum. By alternating hot and cold and wet and dry periods, weathering of the parent material takes place. Bases and silica leach out resulting in a relative accumulation of iron and aluminium. This accumulation will take place at the bottom of the solum. The zone overlying laterite acts as a source. When this zone is only thin this cannot totally explain for the formation of the laterite. Especially in a static profile the iron source is limited.

2. Laterite as a precipitate. The presence of a pallid zone supports the concept of laterite as a precipitate. The upward movement of aluminium and iron is caused by water table fluctuation or capillairy rising. Both mechanisms are however limited to a narrow horizon. By fluctuating groundwater tables over the year, iron precipitates in the top of the fluctuation zone. Iron can originate from the pallid zone underlying the

laterite or from a distant source. When laterite is present on unweathered rock or when the pallid zone is of unsufficient depth this cannot totally explain the formation of the laterite.

3. Laterite consists of cemented weathering products of higher located laterite, the so-called detrital laterite. This is also called false laterite and is found on lower topographical levels than the true laterite (Grandin, 1976).

Formation of iron crusts is usually, by soil scientists, restricted to one of these processes. McFarlane (1976) argues that laterite probably is formed by a combination of above mentioned processes in a static or a downward moving profile.

De Swardt (1964) distinguished two types of laterite in both west and east Africa. " The older is a primary deposit which now forms cappings on erosion remnants and is now separated from the lower laterite by a scarp. The younger is composed largely of rewoked material from the older formation which has been cemented to hard pavement".

This research is focussed on an area close to Kaya (Sanmatenga) in the north-east of Burkina Faso (formerly Upper Volta) in West Africa. In the research area three levels of laterite, rich in secondary iron, occur. The presence of laterite results into bad agriclutural conditions in large areas. In this paper the term 'laterite' or 'iron' crust is used for this ferrugineous material.

Research questions:

* Which processes have successively occured in the research area (based on the theory of McFarlane)?
* Did upward movement of iron occur and is this accompanied by a downward movement of the profile?
* Has laterite been formed as residuum, precipitate or as false laterite?

Laterite caps are present at different levels. Of all these levels undisturbed samples were collected.

* Is it possible to detect from these samples whether the laterite in the lower elevated caps has formed out of weathering products of higher elevated caps?
* Did laterite formation stop at higher locations and are they now only subject to erosion?
* The middle iron crust in the research area clearly consisted of two separated layers. In the upper part iron concretions have been molded together. Did these two layers form in a different way?

Fieldwork in 1994 revealed that lime is present in the area.

* In which horizons is it found?
* Which process is responsible for the lime accumulation?

2 MATERIAL AND METHODS

2.1 Fieldwork and sampling

The studied area is located near the village of Kaya (Sanmatenga) in the North-east of Burkina Faso (formerly Upper Volta) in West Africa. In this area Antebirrimian and Birrimian crystalline formations with strongly weathered plateaus are found. Most of these plateaus are covered with hardened iron (laterite) crusts.
In the research area three levels of iron crusts are present. The iron crusts are presented in Figure 2.1.
An outcrop of granodiorite, assumed to be the parent material, is found in the valley.

Figure 2.1: **Picture of the research area taken from the highest elevated iron crust. Clearly visible are the outcrop of granodiorite (1), the middle one of the iron crusts (2) and the eroded iron gravel (3). Furthermore the lowest elevated iron crust is visible (4).**

At the highest iron crust two pits were described and sampled (no 6 and 7) in a mini catena. At the middle crust, once again in a mini catena, another four (no 2, 3, 4 and 5) profiles were described and sampled, of which of the first two at opposing sites. In the lowest crust no profile was dug and only surface samples collected.

Pit 1, also described and sampled, is located in the centre of the valley where the parent material emerges. Finally some samples were collected from iron crusts in the surrounding area. A cross-section of the research area, with the location of the sampling sites and altitudes, is presented in Annex II. The lowest iron crust is not found in the cross-section.

Figure 2.2: The lowest elevated iron crust

Not having to dig a very deep profile pit and still being able to study the genetical processes over a deep stretch of soil, use was made of the steep slope at the middle crust by digging four pits (2, 3, 4 and 5) close to each other. These pits were dug up till the depth of weathered granodiorite and the elevation of the surface of each description site was measured with a real time kinematics GPS.
Profile descriptions, according to the Guidelines for soil description (FAO, 1990) and making use of the Munsell soil color charts (1975), are presented in Annex III.

2.2 Polarizing microscope observations

Undisturbed soil samples were obtained from the research area. The soil was in a dry state when sampled. The samples were impregnated according to the method of Miedema *et al.* (1974) to preserve the mineralogical composition and field structure. The thin sections were observed under a polarizing optical microscope.

Thin section descriptions were made according to Bullock *et al.* (1985). Use was made of MacKenzie and Guilford (1980) for recognizing minerals under the microscope.

2.3 Chemical analyses

After sampling, the disturbed samples were grinded for chemical analyses.

Mineralogical analysis were performed by X-ray diffraction, sampling period 2,5 hours, using a CEA 15 film. Glycerol was used for sticking the soil sample to the film.
Main (Al, Ca, Fe, Mg, Mn, Si and Ti) and trace elements (Ba, Co, Cr, Cu, Ga, La, Nb, Ni, Pb, Rb, Sr, V, Zn and Zr) were detected by rontgen fluorescency. Grinded samples were put in a stove at a temperature of 100°C. After drying, the samples were cooled and sampled weight was determined. The samples were then ignited in an oven at 900°C. The difference in sample weight is the loss on ignition.
Signals from rontgen fluorescency were transformed to element concentrations by comparison with standards.

3 RESULTS OF FIELDWORK AND SAMPLING

Soil decriptions are presented in Annex III.
Field observations showed in situ formation of the middle and highest elevated iron crust. The middle iron crust consisted of two clearly separate layers. The upper part consisted of cemented iron gravel whereas the lower part revealed in situ formation. The lowest elevated iron crust showed to be a combination of in situ formation and deposition and cementation of iron gravel from higher altitudes.

During the field descriptions, it became clear that strong variations in weathering stage occur within small distances, especially at the middle crust. To capture as many of these variations, both opposing faces of pits 2 and 3 were described. This resulted in 6 sampling sites (2A, 2B, 3A, 3B, 4 and 5) at the middle iron crust.
Although the parent rock was not reached, the oftenly found slightly weathered granodiorite makes its presence in the subsoil of sites 2A, 2B, 3A, 3B, 4 and 5 very likely.
Considering the fast retrograding erosion, it is also likely that the iron crust, now covering site 2A, also used to be on top of sites 2B, 3A, 3B, 4 and 5. Therefore the colluvial material, now covering these sampling sites, is expected to of recent origin.
Finally, by making use of the GPS-data, the observations of the 6 sampling sites were combined with those of site 1 to construct the theoretical profile description from parent rock to iron crust, given below.

I At the bottom of the profile the parent rock, granodiorite, is found.
II The parent rock is covered by a horizon of slightly weathered material. The original granodiorite structure can be recognized but the material has become softer.
III White (brighter than 10YR8/1) sandy loam to sandy clay loam; hard when dry, sticky and very plastic when wet; very few to many, fine to coarse mottles, red (2.5YR5/8) to yellowish red (5YR5/8) and few to many, fine to coarse mottles, yellow (10YR8/8 and 10YR7/8). With decreasing depth, the amount and size of the red to yellowish red and yellow mottles increases, locally the reddish or the yellowish mottles are dominant; very few, fine iron nodules that are reddish brown (2.5 YR4/4) nodules, at the outside and red, yellow and black at the inside; locally very few, very fine, black (N2/) iron manganese nodules; no biological activity i.e. termite activity, worm casts or roots are found present.
IV White (brighter than 10YR8/1) sandy loam to sandy clay loam; hard when dry, firm when moist, slightly sticky and plastic when wet; common to many, medium to coarse, red (2.5YR5/8) and yellowish red (5YR5/8) to strong brown (7.5YR5/6) and very fine to coarse, many to abundant, yellow (10YR7/8), light red (2.5YR7/8) and reddish yellow (7.5YR6/8 and 5YR6/8) to brownish yellow (10YR6/8) mott-

les. By an increase in their size, the area covered by mottles increases with decreasing depth, suggesting growth of the mottles; very few to common, fine to medium nodules that are reddish brown (2.5YR4/4) at the outside and red, yellow and black (N2/) at the inside. With decreasing depth the amount and size of nodules increase. In this horizon locally biological activity (termites, worm casts and roots) is present.

V A red (10R4/6), reddish yellow (5YR7/6) and black iron crust, hardened on exposure to the atmosphere.

Ambrosi *et al.* (1986) (and Ambrosi and Nahon (1986)) also made a description of a lateritic profile in the Diouga area (13°-46'N 0°6'W) in the Northern part of Burkina Faso.
The presence of 6 layers is given although the parent rock and the greenish layer were not reached.

I Parent Rock
II Greenish layer
III Mottled clay layer
IV Soft nodular iron crust
V Hard nodular iron crust
VI Pebbly ferruginous layer

Little differences between both profile descriptions are found, probably due to the gradual boundaries between horizons.
The greenish layer, described by Ambrosi *et al.*, is thought to consist of smectite. A similar layer is absent in the Kaya research area. The only smectite found, are traces just below the soil surface at sampling site 3B (See mineralogical data, Annex VI). However, in 1993, green soil material, consisting of weathered greenschist, a Birrimian rock, and containing smectite clay minerals, was found in the vicinity of the research area (Elkenbracht *et al*, 1994).

Ambrosi *et al.* described the mottled layer as "a horizon were kaolinite domains are dominant in the bottom but toward the top the ferruginous spots or nodules get progressively more numerous and develop at the expense of the grey kaolinitic matrix". Furthermore they described a soft nodular iron crust.
In the Kaya research area two separate layers could be dinstinguished. First a mottled horizon, equivalent to the lower part of the mottled clay layer described by Ambrosi *et al.*. Second a nodular horizon, equivalent to the higher part of the mottled clay layer and soft iron crust described by Ambrosi *et al.*.
Ambrosi *et al.* distinguished a soft nodular iron crust, a hard nodular iron crust and a pebbly ferruginous layer. These were not found in the Kaya area. In the Kaya area the iron crust presented in Figure 3.1 was covered with an iron crust which seemed to consist of detrital coming from higher altitudes.

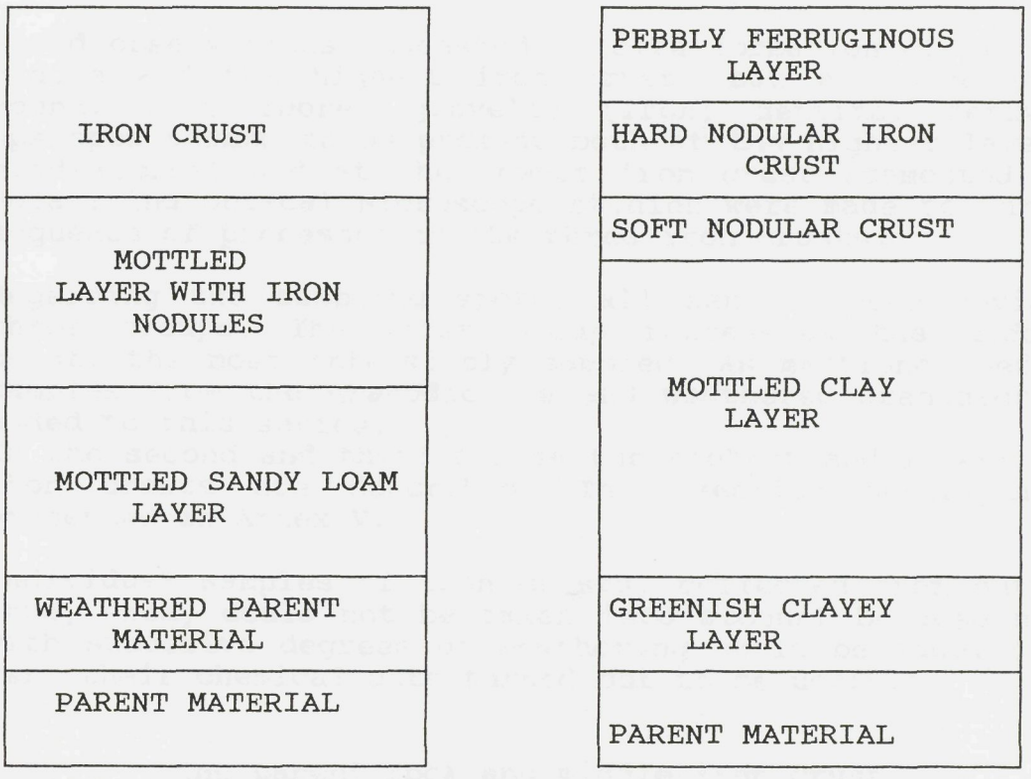

Figure 3.1: **Profiles of lateritic soils. Left profile found in the Kaya area. Right profile found at Diouga by Ambrosi *et al.* (1986).**

Field observations show that the highest elevated iron crust differs from the middle one. Differences are mainly caused by soil colour. The white colour is not found at the sampling sites 6 and 7. A red (2.5 YR4/8) sandy loam to clay is present. No mottling is seen but iron nodules are found. The red colour suggests strong iron impregnation, which masks the presence of mottles. Again in situ formation is suggested.

The lowest elevated iron crust was only sampled superficially so no profile description could be made.

4 RESULTS OF POLARIZING OPTICAL MICROSCOPE OBSERVATIONS

Field observations suggested in situ formation of at least the middle and the highest iron crusts but no sound prove was found. Furthermore, gravelly (iron) detrital derived from upslopes seemed to be present both at the highest layer of the middle crust and at the lowest iron crust (cemented gravel). Polarizing optical microscope studies were made to unravel the sequence of processes in the three iron crusts.

Regarding the sampling spots, all samples were devided into three groups. The first group represents the middle iron crust, the most intensively sampled. As mentioned before, the samples from the granodiorite and weathered granodiorite were added to this series.
In the second and third series the highest and lowest elevated iron crusts are described. Thin section descriptions are presented in Annex V.

Individual samples of iron crusts, collected from outside the study area, could not be taken into account because no series with succesive degrees of weathering could be made. The Howe-ver, their chemical data turned out to be usefull.

4.1 The parent rock and middle iron crust

As described above the parent rock consists of granodiorite.
The granodiorite is made up of quartz, alkali feldspars, green hornblendes, biotite and opaque-iron minerals (see Figure 4.3; horizon I). Concentrations of iron-containing hornblendes, biotite and opaque-iron minerals are located in a clustered distribution pattern.

The fresh granodiorite is covered with a saprolite, developed out of the rock. All minerals in the saprolite are partially or totally weathered. Alkali feldspars demonstrate dotted alteration and the weathering voids are filled with secondary material. Hornblendes display irregular alteration. The weat-hering voids are partially filled with iron.
Biotite shows linear alteration (exfoliation) and the weathe-ring voids are partially filled with dark red iron compounds. Quartz minerals are hardly affected. Original rock structures are not present so the current weathering is not iso-volume-tric.

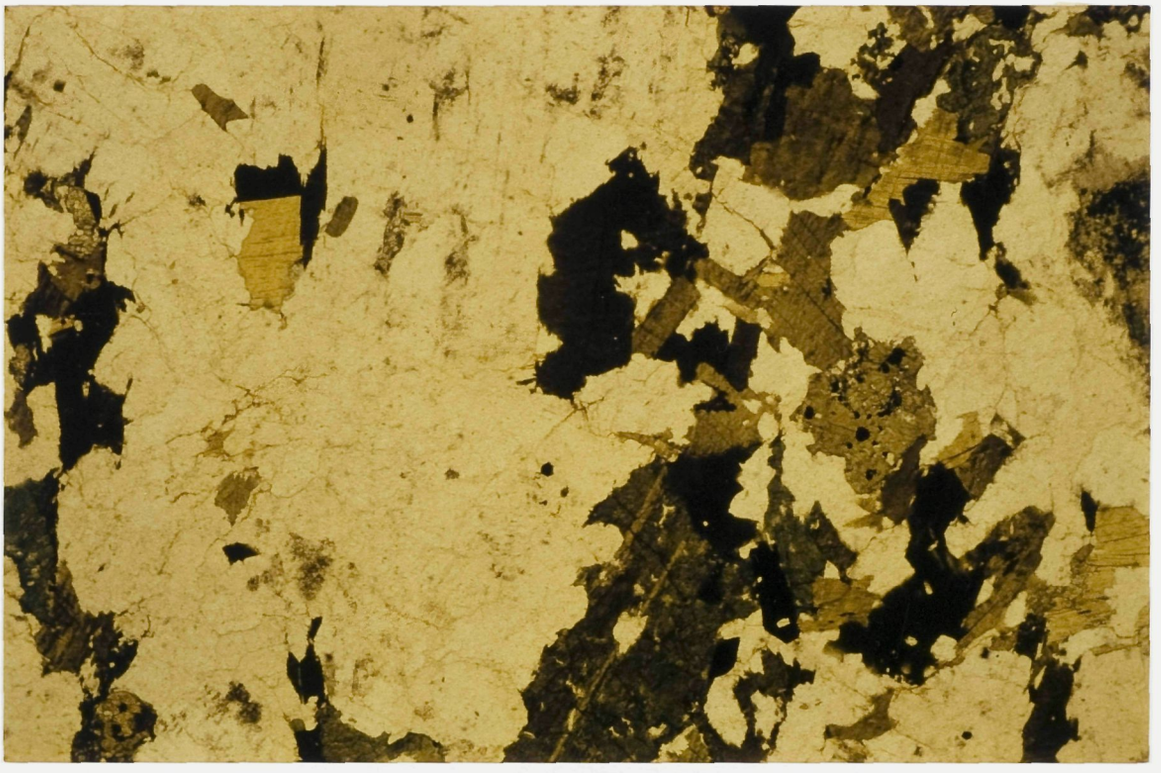

Figure 4.1: Iron-bearing minerals in a clustered distribution patttern present in the parent rock. Plane polarized light (PPL); 1cm = 540um.

The saprolite is devided into a white and yellow coloured saprolite.
The white saprolite is found overlying the weathered granodiorite (see Figure 4.3; horizon II). The coarse fraction (> 5μm) consists of angular quartz grains (up to 1 cm) and clusters of opaque-iron minerals. Many quartz grains are cracked and fall apart into small angular particles. The majority of the fine material (< 5μm) is white and consists of continuous oriented, laminated clay booklets. Based on the internal morphology it is assumed to consist of kaolinite booklets (Bullock *et al.*, 1985). The presence of kaolinite is supported by mineralogical analysis (see Annex VI). Abundant, small (< 3μm), dark grey grains are present giving the fine material an impure character. The grains reflect blue in incident light. The clayey material is thought to be the result of weathering of alkali feldspars, originally present in the parent rock. Clay pseudomorphs after biotite grains are present. No iso-volumetric structures are found.

Two types of clay coatings are distinguished.

I Impure, pale yellowish to white clay coatings (grainy coatings) in voids and as fragmented coatings. They show little birefringence and demonstrate a blueish reflection in incident light. The grainy character and its blueish reflection both in groundmass and pale yellowish clay coatings suggest the occurence of ferrolysis (Brinkman, 19..). Similar phenomena are described by Brinkman *et al.*, 1973). Because coatings are affected by ferrolysis,

clay illuviation must have been active before ferrolysis started. Clay illuviation suggests a climate with a distinct dry season, whereas ferrolysis suggests seasonally wet soils.

II Limpid yellowish clay coatings predominantly in voids. The yellow colour indicates that the coatings contain iron. As the coatings are not grainy they have not been subject to ferrolysis, indicating that they were formed after the process of ferrolysis. Ferrolysis must be a fossil process at this depth.

Orange red iron nodules are present (see Figure 4.3; horizon II) with a diffuse transition to the white saprolite, suggesting in situ nodule formation. In the nodules appreciable amounts of opaque iron minerals, iron-rich claypseudomorph after biotite and hornblende are present, whereas such features occasionally occur in the white coloured saprolite. The formation of the diffuse iron nodules might have taken place around the clustered iron-rich minerals, using the altered iron-rich minerals as cores around which iron accumulation occurs. It is assumed that the nodules are formed due to periodical hydromorph processes.

Iron nodules grow together upon proceeding of the hydromorphic processes and quartz particles are enveloped by iron. Upon weathering of the quartz particles rectangular voids are formed and filled with iron compounds.

With decreasing depth a yellow saprolite occurs (see Figure 4.3; horizon III). It consists predominantly of clay-sized material with many clay booklets, probably formed by weathering of alkali feldspars. In this fine textured groundmass big quartz grains (up to 1 cm), totally weathered biotite and hornblendes as well as fresh opaque iron minerals are present. However, quartz minerals are hardly affected by weathering. Micromorphological observations indicate that the yellow saprolite is built up exactly like the white saprolite but the fine material of the yellow saprolite contains some homogeneously distributed iron.
Yellow and white saprolite can be found next to each other. With decreasing depth the amount of the yellow saprolite increases. Both observations suggest better drainage conditions in the yellow saprolite.
Yellowish limpid clay coatings are found in the yellow saprolite.

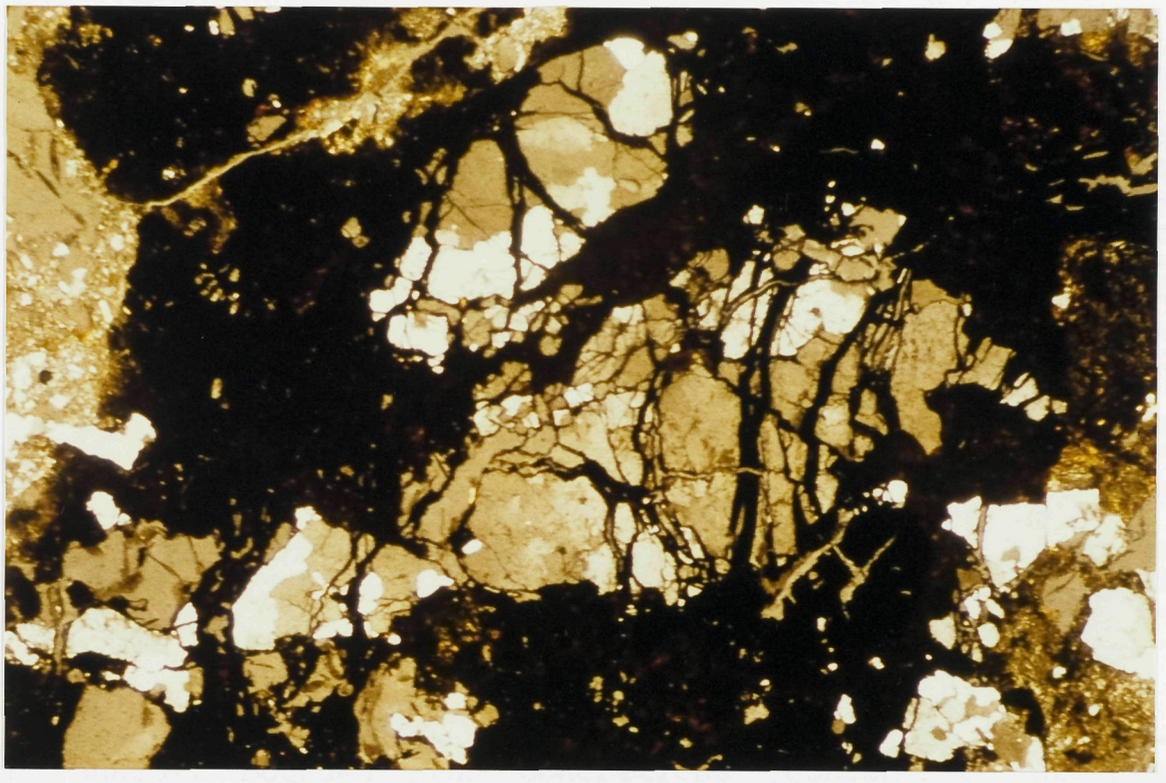

Figure 4.2: Occurence of iron accumulated around the clusters of iron-rich minerals as found in the parent rock. Different iron-rich areas have grown together, enveloping quartz grains. Upon ongoing weathering and cracking of the minerals iron compounds filled up the cracks. Weathering proceeded and some parts of the original quartz grain totally disappeared. Crossed polarized light (XPL); 1cm = 400um.

Field observations show that the iron crust at the surface of this site consists of two clearly separate layers. Micromorphological observations of the lower demonstrate that it mainly consists of yellow saprolite with traces of white saprolite. Furthermore aggregates, consisting of fine (50-150μm) quartz particles and reddish clay material, are observed (see Figure 4.3; horizon IV). The scattered occurence of individual small quartz grains in the reddish clay groundmass suggests that the original primary minerals are totally weathered and transformed to clay. As a result the quartz grains are residual enriched and mechanically fall apart into smaller constituents.
Many fragmented, limpid, red, clay coatings (papules, Brewer, 1964) are present in the red aggregates. They are absent in both white and yellow saprolite suggesting that clay illuviation has taken place before the internal fabric of the groundmass has been disturbed by physicogenic or biogenic processes and that these aggregates are inherited.

With decreasing depth a third type of clay coatings is found:
III Limpid red clay coatings. Locally these red coatings can be covered with the previous mentioned (II) yellow coatings. This sequence of coatings can be found both in the yellow and white saprolite as well as between the yellow saprolite and red material. This indicates that red coating-formation started after formation of yellow and white saprolite and after the incorporation of red aggregates. In addition this indicates that the red coatings were formed before the yellow coatings were deposited. Finally it indicates that red coatings have been formed after the process of ferrolysis ended, so it confirms that ferrolysis is a fossil process.
In situ reddish clay coatings are present in cracks, which form the boundary between red aggregates and yellowish saprolite. This indicates that red papules in the red soil are older than the in situ red coatings.
It is speculated that the reddish soil aggregates are remnants of a red soil, originally overlying the yellow saprolite and formed from that saprolite due to tension in the soil material, resulting in fine quartz grains and fragmented clay coatings.

The upper part of the iron crust mainly constists of spherical, sharply bounded iron concretions (concentric internal fabric) (see Figure 4.3; horizon V). Occasionally quartz or other primary minerals are present. Intergranular voids between the concretions are partially filled with iron. These observations confirm the field hypothesis that the iron crust consists of two layers which genetically differ. The lower part is considered a remnant of a reddish soil of unknown thickness overlying the yellowish saprolite and genetically related with this saprolite. The majority of the reddish soil has been eroded because in the field the red soil material was not observed as a continuous soil horizon but as remnants in the yellowish saprolite. Micromorphology confirms these observations. After erosion of the red soil, iron concretions (gravel) has been deposited on the remnants of the red soil. It is speculated that the iron gravel originates from older iron crusts, present at higher elevated positions in the landscape.

Occasionaly, next to the yellow and white saprolite, a brown-red clayey material with a different b-fabric is found. It contains small quartz grains and micas. It contains organic matter resulting in a different colour. It has a granular microstructure. This material is supposed to originate from biological activity e.g. termite or worm activity.

In situ lime accumulations are present in cracks in the yellowish and white saprolite and also occur on yellowish clay coatings. Locally lime accumulations are found in voids in the red material. Observations indicate that the lime formations occur after formation of both saprolites and red soil aggregates and after all clay illuviation processes. It appears to be the youngest phase of soil formation. The origin and genesis of the secondary lime cannot be deduced from micromorpholo-

gical observations. From chemical analyses it is concluded that the granodiorite is the source of secondary lime enrichment.

Hor. V: Upper part of the iron crust with inherited spherical, sharply bound iron gravel and intergranular voids filled with iron.
Hor. IV: Lower part of the iron crust with a yellow saprolite, traces of a white saprolite and the presence of a red soil aggregates with red fragmented clay coatings. Presence of in situ limpid red clay coatings.
Hor. III: White saprolite (occasionally subject to ferrolysis) and yellow saprolite with limpid yellow clay coatings. With decreasing depth more yellow saprolite. Presence of iron nodules. Locally termite activity and lime are present.
Hor. II: White saprolite with dusty clay coatings locally subject to ferrolysis and limpid yellow coatings not subject to ferrolysis. Presence of iron nodules.
Hor. I: Parent rock (granodiorite).

Figure 4.3: Micromorphological description of the middle iron crust

Micromorphological observations indicate that the following soil forming processes have taken place succesively.

1 Isovolumetric weathering of primary minerals in the granodiorite and formation of secondary minerals (clay-pseudomorphs **after** primary minerals, mainly feldspars); forming the yellow saprolite.
2 Occurence of hydromorphic processes in the porous zones of the yellow saprolite, resulting in the formation of white zones.
3 Clay illuviation in more porous zones in the white saprolite leading to coating type I.
4. Occurence of ferrolysis in the white saprolite and formation of iron nodules around existing iron cores.
5. Formation of red soil material from the yellow saprolite and overlying the yellow saprolite.
6. Clay illuviation and rubifaction in the red soil and formation of red coatings.
7. Fragmentation of coatings and formation of papules.

8. Transportation of red soil aggregates into the yellow saprolite.
9 Clay illuviation and formation of red and yellow clay coatings respectively type III and II.
10. Erosion of the red soil horizon
11. Deposition of detrital iron gravel.
12. Accumulation of lime.

4.2 The highest elevated iron crust

The highest elevated iron crust consists of two materials:

i A dark red saprolite with big quartz grains (600-800μm), clay pseudomorphs after biotite and iron pseudomorphs after hornblendes. The saprolite is partially iso-volumetric weathered and is totally impregnated with iron. With increasing depth the saprolite-like structure disappears. Dark red iron nodules are found, in which angular shaped cavities occur occasionally containing quartz grains. Such quartz grains are generally smaller than the cavities indicating a pellicular alteration which means that weathering affected the outer margins of the quartz. It is unlikely that this phenomenon resulted from thin section preparation because the outer bounderies of the quartz grains are smooth. Occasionally quartz grains have completely disappeared. A frame work or iron remains. This indicates that dissolution of quartz minerals continuous after impregnation with iron.

ii A light red clayey soil material. Saprolite structures are absent. The light red material dominantly consists of clay booklets, probably derived from totally weathered feldspars, and furthermore consists of biotite and quartz grains. The clay booklets are smaller than those found in the dark red saprolite. Few quartz grains are found, with smaller sizes than those observed in the dark red saprolite. With decreasing depth the soil material becomes more reddish.

Obviously both materials have the same mineralogical composition (quartz grains and micas) indicating a similarity in respect to parent material. Based on the differences in size of the primary and secondary minerals, and on the differences in internal fabric, the light red material is thought to be more strongly weathered.

It is concluded that the highest iron crust is formed in situ. Iron-rich nodules are formed in the same way as those present in the middle iron crusts. The iron-rich nodules are usually accompanied by a material with the same composition of primary minerals. However the degree of weathering is different. Both materials have been derived from the same parent material (granodiorite). Differences in macroporosity of the rock causes preferent waterways which in turn cause different degrees of weathering at macro and micro scale.

Also at the foot of the highest elevated iron crust samples were taken (no. 6). Optical studies reveal that the samples differ from the material described above. Instead it showed a groundmass consisting of:

I Dark red, sharpley bounded iron gravel of alternating mineralogical composition (in terms of amounts of biotite and quartz) and size (50μm-2cm).

II A heterogeneous yellow-red soil material, between the iron gravel, with big quartz minerals (300μm). In this soil material, layers of pure iron compounds are found.
The different internal fabric of iron gravel, their angular shape and its sharp bounderies, indicate that the material found in this thin section has not been formed in situ.
The heterogeneous yellow-red material is impregnated and cemented by iron and overlies a groundmass where iron gravel is commonly found. The dark red iron gravel has a similar b-fabric as the dark red iron nodules in the dark red saprolite found at the top of the iron crust.

Spherical to elipsical, white, clay aggregates are found. This white material is grainy and reflects blue under incident light, indicating that this material may have been subject to ferrolysis. Small (50μm) quartz grains are found in the clayey material. Within the white aggregates, red iron droplets in alternating amounts are found and iron is also surrounding the aggregates. It seems that erosion material, consisting of the white saprolite and quartz grains, is cemented by iron. The cause of the white saprolite transport is not exactly known. The spherical to elipsical shape suggests both biological activity (termites) and erosion (at heigh altitudes) and deposition (at lower altitudes).

It is concluded that in situ material at the foot of the iron crust can have be covered by detrital material consisting of iron gravel from heigher altitudes.

4.3 The lowest elevated iron crust

The lowest elevated ironcrust consists of:
I A white saprolite consisting of white clay-booklets and coarse quartz grains (250-500μm). In the white saprolite light yellow coatings are found. Both saprolite and light yellow coatings are subject to ferrolysis. Locally aggregates of white saprolite are found.

II A yellow saprolite consisting of clay booklets and coarse quartz grains (up to 500μm). Locally aggregates of yellow saprolite are present.

III Dark red ferric nodules. Occasionally the dark red ferric nodules seem to be formed in situ i.e. micromorphological observations make clear that the ferric nodules and the adjacent saprolite have the same mineralogical composition regar-

ding clay booklets and size of quartz grains. The transition from the dark red ferric nodules to the white saprolite is diffuse. However dark red ferric nodules with a sharp transition to the saprolite are found indicating that these ferric nodules are detrital.

IV Iron gravel with a b-fabric differing from the ferric nodules and the saprolite described above. The transition between iron gravel and adjacent material is sharp.

Micromorphological observations indicate both in situ formation of the lowest elevated iron crust and inheritance of features described above. Dark red ferric nodules seem to be formed in situ when mineralogical composition stems with the mineralogical composition of the white saprolite and when the transition between both materials is diffuse.
Aggregates of white and yellow saprolite and dark red ferric nodules with sharp transitions to the adjacent material seem to be inherited from higher altitudes. The locally found sharp edged ferric nodules also suggest an inherited origin.
The process of in situ crust formation is similar to that in the middle crust, as described in 4.1. Furthermore, detrital derived from higher altitudes seems to deposit dominantly at locations rich in iron.

5 CHEMICAL RESULTS

After substracting the weight percentage of the loss on ignition from the data obtained by rontgenfluorescence, these data are recalculated again to 100%, as follows:

$$100/(W_1 - W_2) \qquad (5.1)$$

in which:

W_1 = the sum of the weight percentages of all elements and

W_2 = weight percentage of the 'loss on ignition'

The corrected chemical data are presented in Annex VII A (main elements) and VII B (trace elements).
All concentrations are expressed as percentage of the total weight, assuming all elements to be present as oxides.
The weight percentages of four major elements (SiO_2, TiO_2, Fe_2O_3 and Al_2O_3) are presented in Figures 5.1-5.6, and are discussed below.
In the granodiorite and the slightly weathered granodiorite besides the above mentioned elements Na_2O, K_2O, BaO, MgO, MnO and CaO are found in significant amounts. These elements are hardly found in the other samples.

Field and micromorphological observations indicated the local presence of lime throughout the sampling sites 2A, 2B, 3A, 3B, 4 and 5 at the transition from red iron mottles or nodules to the white clayey material. Due to the size of the soil samples these locally high lime concentrations are reduced to the extend that the chemical data do not show the presence of lime. However it becomes clear that the granodiorite must be the origin of the local lime enrichment.

In the following paragraphs the terms absolute and relative enrichment or accumulation mean:

Relative enrichment or accumulation: increase in weight percentage of an element due to a nett loss of other elements.
Absolute enrichment or accumulation: increase in weight percentage of an element due to an influx of the element from adjacent areas.

The parent material, granodiorite, indicates a rather homogeneous occurence of TiO_2%. Micromorphological studies revealed nearly only in situ pedogenetic processes, meaning no mechanical redistribution of TiO_2. As TiO_2 is also considered rather inert, i.e. neither subject to eluviation nor illuviation, the ratio of an element weight% : TiO_2% in this case indicates whether absolute or relative enrichment of that element has taken place. An increase in the ratio suggests an absolute accumulation, a decrease a nett leaching. An increasing TiO_2% is explained by relative enrichment.

In the discussion of the figures five different processes are recognized. The processes of iron- and clay illuviation and ferrolysis have already been observed during the micromorphological studies. Chemical data expressed leaching of Na_2O, K_2O, BaO, MnO, MgO and CaO and the process of ferralitization. The effects of these five processes on the change in weight percentages of the four major elements are given in Table 5.1.

Table 5.1: The effects of various processes on the concentration of aluminium, iron and silicium and titane oxides in the soil.

PROCESS	Al_2O_3%	Fe_2O_3%	SiO_2%	TiO_2%
Leaching of Na_2O, K_2O, BaO, MnO, MgO and CaO	+/-	+/-	+/-	+/-
Ferralitization	+/-	+/-	-	+/-
Ferrolysis	-	-	+/-	+/-
Iron illuviation	-/-	+	-/-	-/-
Clay illuviation	+	-/-	+	-/-

\+ = absolute enrichment
\- = absolute loss
+/- = relative enrichment (loss of other elements)
-/- = relative loss (enrichment with other elements)

Information on sample numbers, sample site and altitude of sampling are presented in Annex IV. Sample numbers increase with increasing altitudes.

5.1 Fe_2O_3 versus TiO_2

The weight percentages of Fe_2O_3 versus TiO_2, after correction for loss on ignition are found in Figure 5.1.

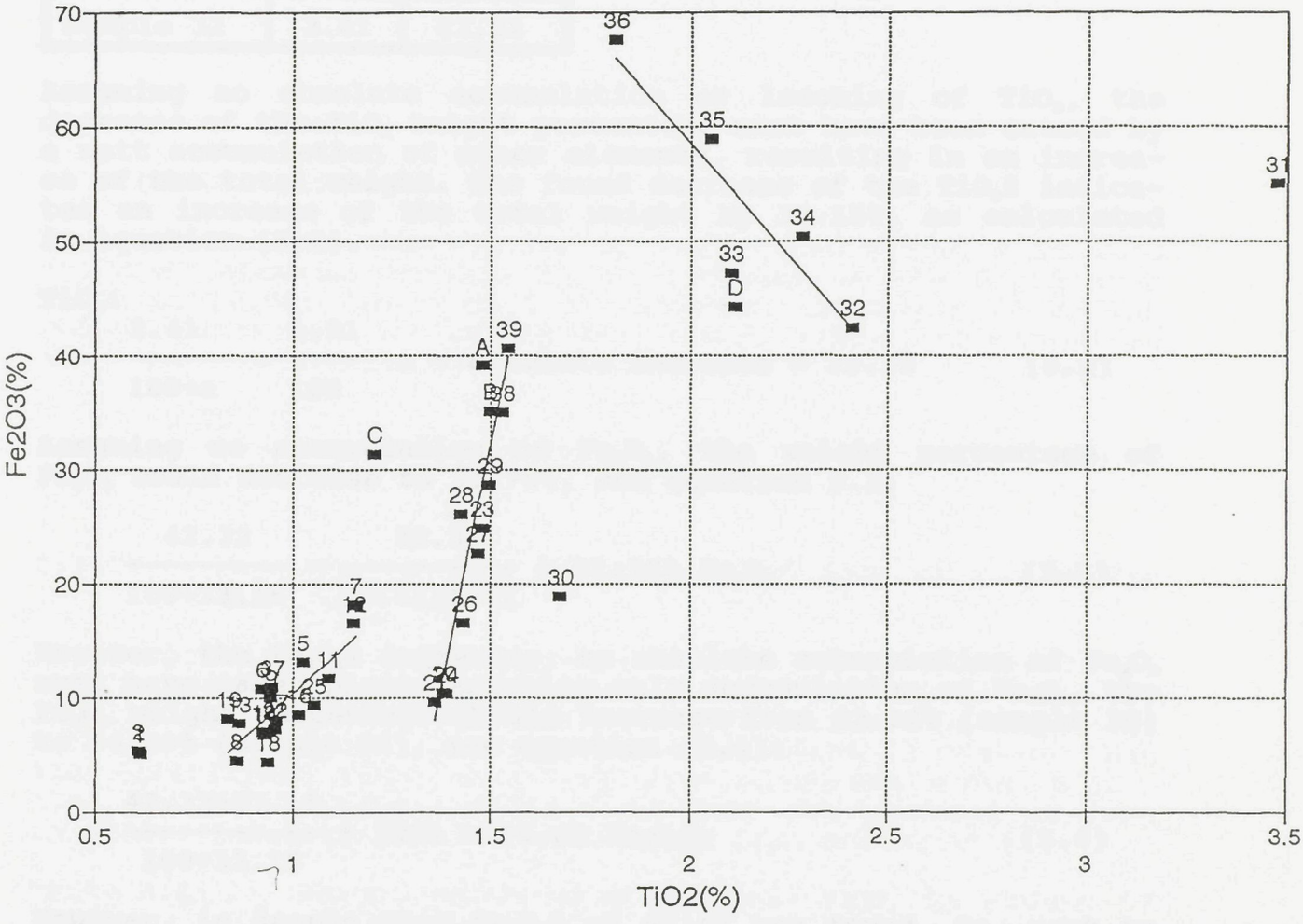

Figure 5.1: Weight percentage Fe_2O_3 versus weight percentage TiO_2

5.1.1 Fe_2O_3 versus TiO_2 in the highest elevated iron crust

The x-coefficient of the regression line (see Figure 5.1) of the samples 32, 33, 34, 35 and 36 is -39.7, indicating an increase of the Fe_2O_3-content with a decreasing TiO_2 content. All calculated x-coefficients can be found in Annex VIII. When moving up in the iron crust, e.g. from sample 32 to 36, the TiO_2 weight percentage decreases.

Table 5.2: Weight percentages TiO_2 and Fe_2O_3 in sample 36 and sample 32

	TiO_2%	Fe_2O_3%
Sample 36	1.81	67.47
Sample 32	2.41	42.32

Assuming no absolute accumulation or leaching of TiO_2, the decrease of the TiO_2 weight percentage must have been caused by a nett accumulation of other elements, resulting in an increase of the total weight. The found decrease of the TiO_2% indicates an increase of the total weight by 33.15%, as calculated in equation (5.2).

TiO_2:

$$\frac{2.41}{100+a} = \frac{1.81}{100} \qquad a = \text{absolute increase} = 33.15 \qquad (5.2)$$

Assuming no accumulation of Fe_2O_3, the weight percentage of Fe_2O_3 would decrease to 31.78%, see equation 5.3.

$$\frac{42.32}{100+33.15} = \frac{42.32}{2.41/1.81} = 31.78\%\ Fe_2O_3 \qquad (5.3)$$

However, the Fe_2O_3% increases, so absolute accumulation of Fe_2O_3 must have taken place. Assuming only accumulation of Fe_2O_3, the Fe_2O_3 weight percentage should increase from 42.32% (sample 32) to 56.69% (sample 36), see equation (5.4):

$$\frac{42.32+33.15}{100+33.15} * 100\% = 56.69\ Fe_2O_3\% \qquad (5.4)$$

However, in sample 36 a Fe_2O_3% of 67.47 was found. So, next to an accumulation of Fe_2O_3, other elements must have leached out.

5.1.2 Fe_2O_3 versus TiO_2 in the middle iron crust

The x-coefficient of the regression line of the Fe_2O_3 and TiO_2 concentrations of samples 20, 21, 23, 24, 26, 27, 28, 29, 38, 39, A and B is 173,8. Contrary to the highest elevated iron crust, an increase in the TiO_2 weight percentage is accompanied by an increase of the Fe_2O_3 weight percentage.

When getting closer to the surface of the crust, from sample 21 to sample 29, the TiO_2% increases slightly. Again assuming no nett loss or accumulation of TiO_2, the increase of TiO_2% must have been the result of a nett loss of other elements. The decrease of the TiO_2 weight percentage from 1.36 to 1.50 indicates a nett loss of 9.33% in total weight (equation 5.5).

Table 5.3: Weight percentages TiO_2 and Fe_2O_3 in sample 29 and sample 21

	TiO_2%	Fe_2O_3%
Sample 29	1.50	28.61
Sample 21	1.36	9.52

TiO_2:

$$\frac{1.36}{100+a} = \frac{1.50}{100} \qquad a = -9.33 \qquad (5.5)$$

When no absolute accumulation of Fe_2O_3 takes place, this loss of other elements results in an increase of the Fe_2O_3% from 9.52% to 10.50% (equation 5.6). However, in sample 29 a Fe_2O_3 weight percentage of 28.61% was found, again indicating an absolute accumulation of iron.

$$\frac{9.52}{100-9.33} * 100 = 10.5\%\ Fe_2O_3 \qquad (5.6)$$

5.1.3 Fe_2O_3 versus TiO_2 in the mottled zone of the middle iron crust

The x-coefficient of the regression line (Fe_2O_3% versus TiO_2%) of the samples 5, 6, 7, 8, 9, 10, 11, 12, 13, 14, 16, 17, 18, 19, 22, 25 and 37 is 31.37 indicating an increase of the Fe_2O_3% with an increase of the TiO_2%. The coefficient is smaller than the coefficient found with the data discussed under 5.1.2, i.e. the delta Fe_2O_3% : delta TiO_2% does not increase as fast as above. Indicating a less pronounced Fe_2O_3 accumulation.

Table 5.4: Weight percentages TiO_2 and Fe_2O_3 in sample 17 and sample 8.

	TiO_2%	Fe_2O_3%
Sample 17	0.96	8.04
Sample 8	0.85	4.41

The increase of the TiO_2% from 0.85 to 0.96 suggests a nett loss of 11.46 in total weight (equation 5.7).

TiO_2:

$$\frac{0.85}{100+a} = \frac{0.96}{100} \qquad a = -11.46\% \qquad (5.7)$$

This loss in total weight would result in an increase of the

Fe_2O_3 weight percentage from 4.41% to 4.98% (equation 5.8). However, a Fe_2O_3% of 8.04 was found. So, next to a loss of other elements, an absolute accumulation of Fe_2O_3 must have taken place.

$$\frac{4.41}{100-26.09} * 100 = 4.98\%\ Fe_2O_3 \qquad (5.8)$$

5.2 AL_2O_3 versus TiO_2

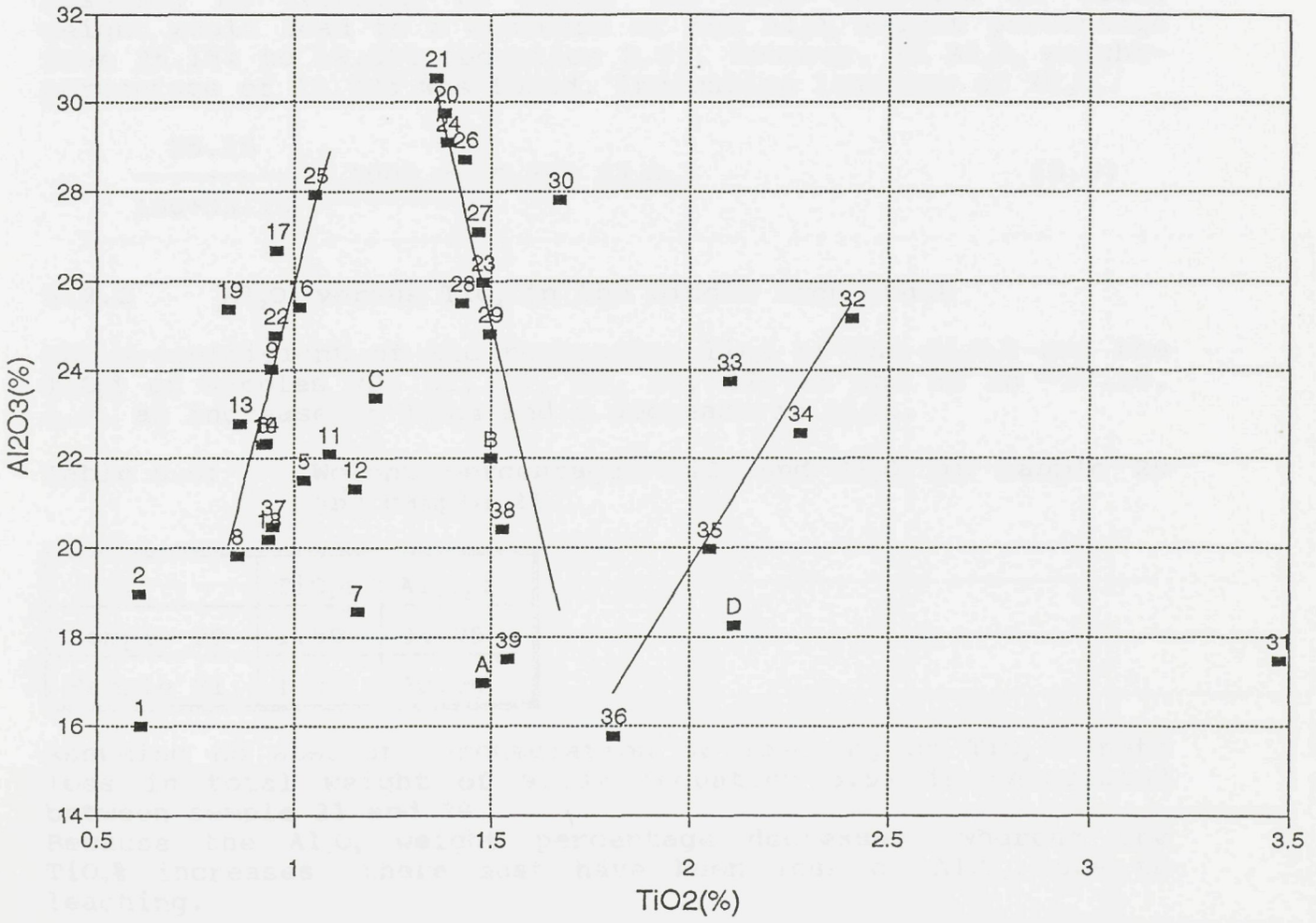

Figure 5.2: Weight percentage Al_2O_3 versus weight percentage TiO_2.

5.2.1 Al_2O_3 versus TiO_2 in the highest elevated iron crust

The x-coefficient of the regression line of the Al_2O_3% and the TiO_2% of samples 32, 33, 34, 35 and 36 is 14,68%. When moving to the surface of the iron crust, a decrease of the TiO2% is accompanied by a decrease in the Al_2O_3 weight percentage.

As decribed for Fe_2O_3 versus TiO_2, the decrease in TiO_2 weight percentage (between sample 32 and 36) is the result of a nett increase in total weight of 33.15% (equation 5.2).

Table 5.5: Weight percentages TiO_2 and Al_2O_3 in sample 36 and sample 32.

	TiO_2%	Al_2O_3%
Sample 36	1.81	15.78
Sample 32	2.41	25.15

Assuming no leaching of Al_2O_3, the nett increase in total weight would lead to a decrease of the Al_2O_3 weight percentage from 25.15% to 18.89% (equation 5.9). However, an Al_2O_3 weight-percentage of 15.78% was found, indicating leaching of Al_2O_3.

$$\frac{25.15}{100+33.15} * 100\% = 18.89\%\ Al_2O_3 \qquad (5.9)$$

5.2.2 Al_2O_3 versus TiO_2 in the middle iron crust

The x-coefficient of the regression line of the Al_2O_3% and the TiO_2% of samples 20, 21, 23, 24, 26, 27, 28 and 29 is -37.10, i.e. an increase in TiO_2% and a decrease in Al_2O_3.

Table 5.6: Weight percentages TiO_2 and Al_2O_3 in sample 29 and sample 21.

	TiO_2%	Al_2O_3%
Sample 29	1.50	24.79
Sample 21	1.36	30.54

Assuming no absolute accumulation or leaching of TiO_2 a nett loss in total weight of 9.33% (equation 5.5) is calculated between sample 21 and 29.
Because the Al_2O_3 weight percentage decreases, whereas the TiO_2% increases, there must have been loss of Al_2O_3, due to leaching.

5.2.3 Al_2O_3 versus TiO_2 in the mottled zone of the middle iron crust

The x-coefficient of the regression line of the Al_2O_3% and the TiO_2% of samples 6, 8, 9, 10, 13, 14, 16, 17, 22 and 25 is 34.88. So an increase in the TiO_2% is accompanied by an increase in Al_2O_3%. The increase in TiO_2%, between the samples 8 and 17, results from a loss of total weight of 11.46% (equation 5.7).

Table 5.7: Weight percentages TiO_2 and Al_2O_3 in sample 17 and sample 8.

	TiO_2%	Al_2O_3%
Sample 17	0.96	26.67
Sample 8	0.85	19.83

Assuming no leaching of Al_2O_3 this would result in an increase in the Al_2O_3 weight percentage from 19.83 to 22.40% (equation 5.10). A weight percentage of 26.67 was found for Al_2O_3, indicating absolute accumulation of Al_2O_3.

$$\frac{19.83}{100-11.46} * 100\% = 22.40\% \; Al_2O_3 \qquad (5.10)$$

5.3 SiO_2 versus TiO_2

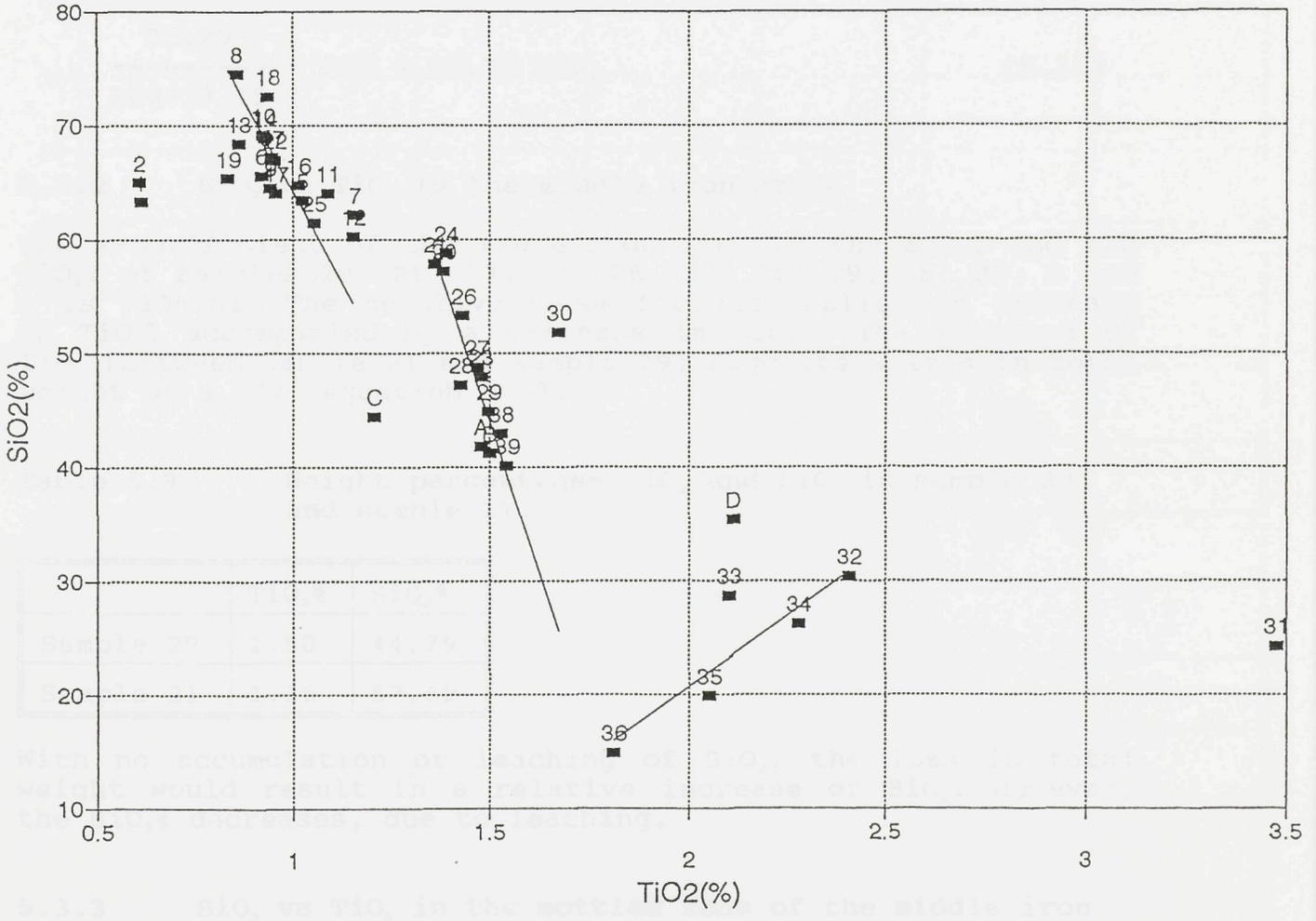

Figure 5.3: Weight percentage SiO_2 versus weight percentage TiO_2

5.3.1 SiO_2 vs TiO_2 in the highest elevated iron crust

The x-coefficient of the regression line of the SiO_2% and the TiO_2% of samples 32, 33, 34, 35 and 36 is 24.96. A decrease in TiO_2 is accompanied by a decrease in SiO_2. As described above, the total weight has increased with 33.15% (equation 5.2). The increase is caused by leaching of Al_2O_3 and absolute accumulation of Fe_2O_3.

Table 5.8: Weight percentages TiO_2 and SiO_2 in sample 32 and sample 36.

	TiO_2%	SiO_2%
Sample 36	1.81	14.79
Sample 32	2.41	30.29

Assuming no loss of SiO_2, the increase in total weight would result in a SiO_2% of 22.75 (equation 5.11). However, a weight percentage of 14.79 was found, indicating leaching of SiO_2.

$$\frac{30.29}{100+33.15} * 100 = 22.75\ SiO_2 \qquad (5.11)$$

5.3.2 SiO_2 vs TiO_2 in the middle iron crust

The x-coefficient of the regression line of the SiO_2% and the TiO_2% of samples 20, 21, 23, 24, 26, 27, 28, 29, 38, 39, A and B is -105.51. The negative x-coefficient implies an increase in TiO_2% accompanied by a decrease in SiO_2%. The increase of TiO_2 (between sample 21 and sample 29) suggests a loss in total weight of 9.33% (equation 5.5).

Table 5.9: Weight percentages TiO_2 and SiO_2 in sample 29 and sample 21.

	TiO_2%	SiO_2%
Sample 29	1.50	44.79
Sample 21	1.36	57.69

With no accumulation or leaching of SiO_2, the loss in total weight would result in a relative increase of SiO_2. However, the SiO_2% decreases, due to leaching.

5.3.3 SiO_2 vs TiO_2 in the mottled zone of the middle iron crust

The x-coefficient of the regression line of the SiO_2% and the

T
6
a
T
w

T

A
i
H

5

Fi

TiO_2% of samples 8, 9, 10, 14, 16, 17, 18, 22, 25 and 37 is -63.79. When moving closer to the surface the TiO_2% increases and the SiO_2% decreases. As described above this increase in TiO_2% from 0.85 to 0.96 is the result of a nett loss in total weight of 11.46% (equation 5.7)

Table 5.10: Weight percentages TiO_2 and SiO_2 in sample 17 and sample 8.

	TiO_2%	SiO_2%
Sample 17	0.96	63.91
Sample 8	0.85	74.48

Assuming no leaching or absolute accumulation of SiO_2, the loss in total weight would result in an increase of the SiO_2%. However, the SiO_2% decreases, indicating leaching of SiO_2.

5.4 SiO_2 versus Al_2O_3

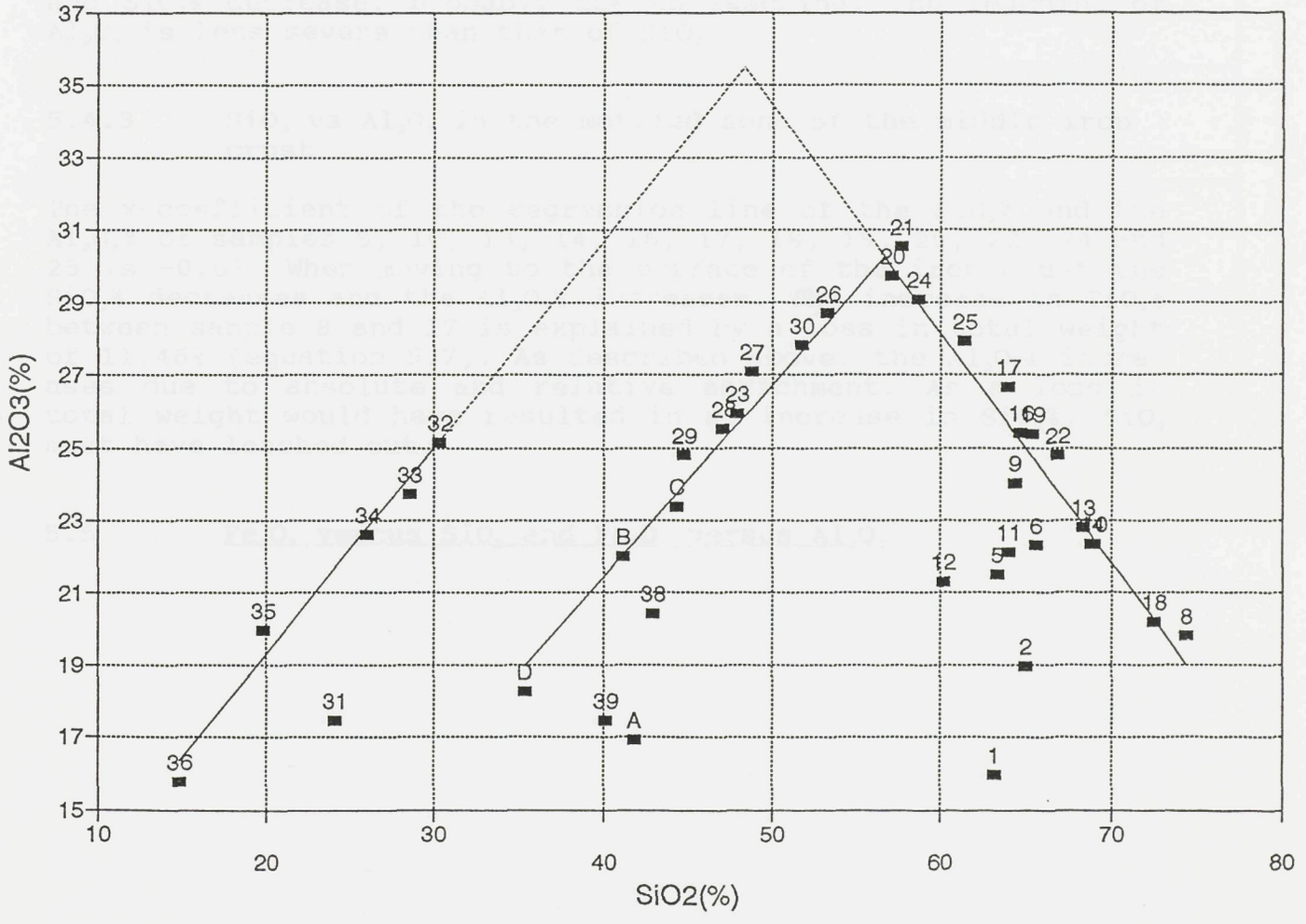

Figure 5.4: Weight percentage SiO_2 versus weight percentage Al_2O_3.

5.4.1 SiO_2 vs Al_2O_3 in the highest elevated iron crust

The x-coefficient of the regression line of the SiO_2% and the Al_2O_3% of samples 32, 33, 34, 35 and 36 is 0.57. Both the weight percentage of SiO_2 and the weight percentage of Al_2O_3 decrease when moving higher up in the profile.
The graphs SiO_2 versus TiO_2 and Al_2O_3 versus TiO_2 indicated leaching of both SiO_2 and Al_2O_3 when moving up in the highest elevated iron crust.
The x-coefficient indicates that the dependent value (Al_2O_3) lowers with 0.57 when the independent value (SiO_2) lowers with 1 i.e. SiO_2 leached more than Al_2O_3.

5.4.2 SiO_2 vs Al_2O_3 in the middle iron crust

The x- coefficient of the regression line of the SiO_2% and the Al_2O_3% of samples 20, 21, 23, 26, 27, 28, 29 and 30 is 0.43 i.e. when the SiO_2% decreases with 1 the Al_2O_3 decreases with 0.43. When going up in the profile from sample 21 to 29, the TiO_2% increases, indicating a loss in total weight. Both Al_2O_3% and SiO_2% decrease, probably due to leaching. The leaching of Al_2O_3 is less severe than that of SiO_2.

5.4.3 SiO_2 vs Al_2O_3 in the mottled zone of the middle iron crust

The x-coefficient of the regression line of the SiO_2% and the Al_2O_3% of samples 8, 10, 13, 14, 16, 17, 18, 19, 20, 22, 24 and 25 is -0.63. When moving to the surface of the iron crust the SiO_2% decreases and the Al_2O_3% increases. The increase in TiO_2% between sample 8 and 17 is explained by a loss in total weight of 11.46% (equation 5.7). As described above, the Al_2O_3% increases due to absolute and relative enrichment. As a loss in total weight would have resulted in an increase in SiO_2%, SiO_2 must have leached out.

5.5 Fe_2O_3 versus SiO_2 and Fe_2O_3 versus Al_2O_3

Fe2O3(%)

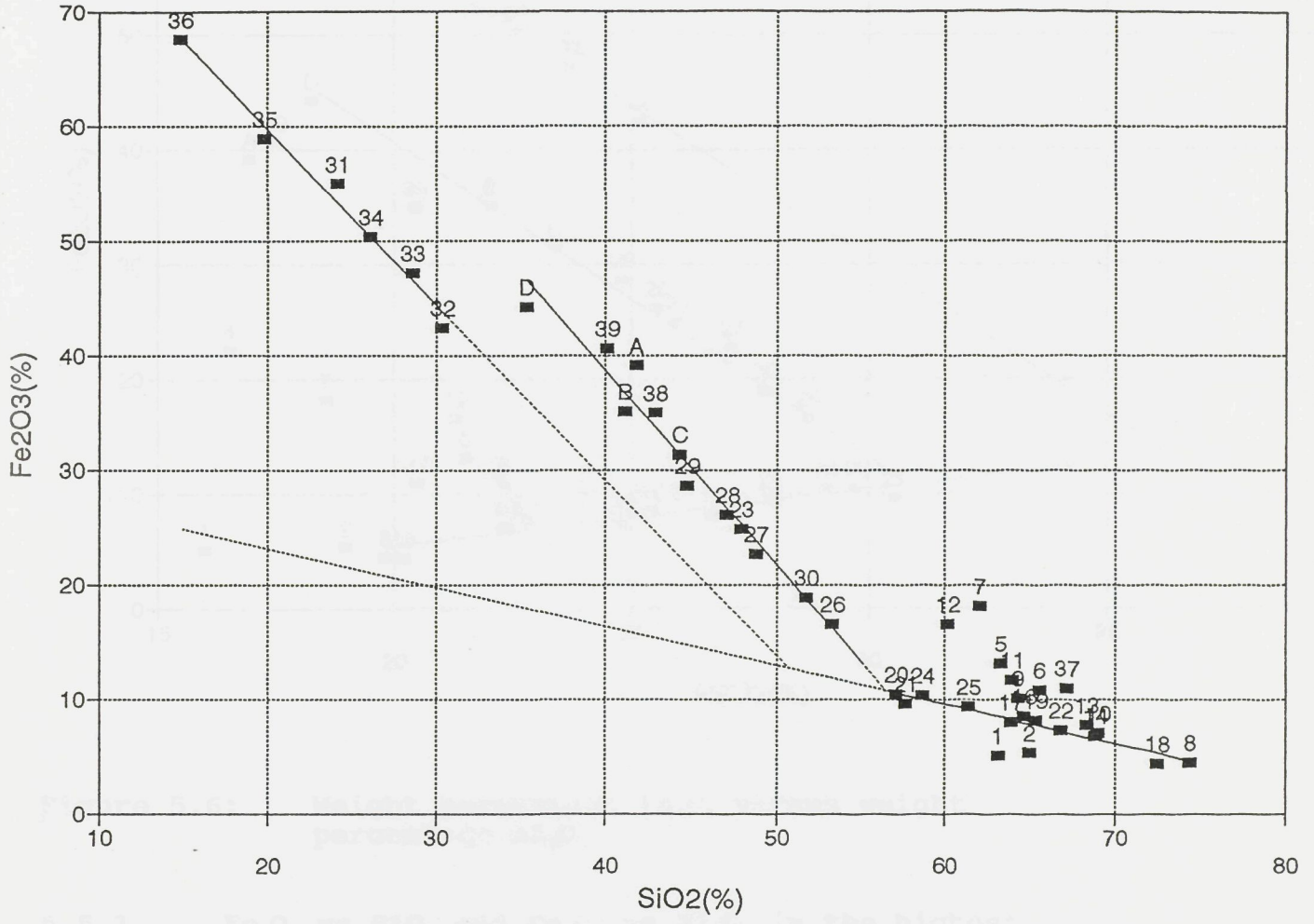

Figure 5.5: Weight percentage Fe_2O_3 versus weight percentage SiO_2

Fi

5

Wh
in
de
Fe
Th
3.
th
A
in

5

Th

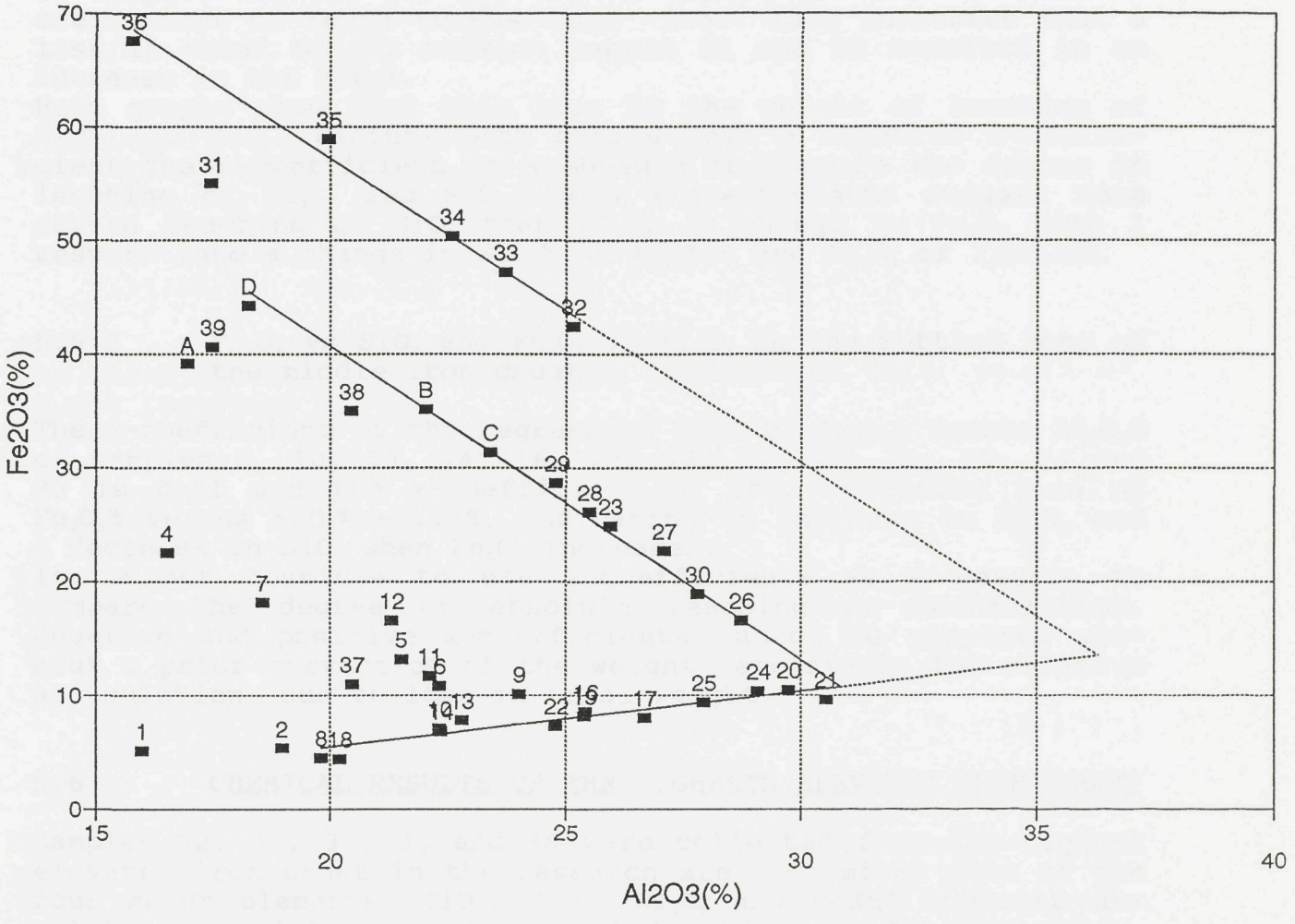

Figure 5.6: **Weight percentage Fe_2O_3 versus weight percentage Al_2O_3**

5.5.1 Fe_2O_3 vs SiO_2 and Fe_2O_3 vs Al_2O_3 in the highest elevated iron crust

When moving up in the highest elevated iron crust the Fe_2O_3% increases and the weight percentages of both Al_2O_3 and SiO_2 decrease. This is explained by an absolute accumulation of Fe_2O_3 and nett loss, by leaching, of Al_2O_3 and SiO_2.
The x-coefficient of the regression line of samples 32, 33, 34, 35 and 36 of the Fe_2O_3% versus the SiO_2% is -1.35, that of the Fe_2O_3% versus the Al_2O_3% is -6.68.
A set increase in Fe_2O_3 is accompanied by a Fe_2O_3/1.53 decrease in SiO_2 and by a Fe_2O_3/2.68 decrease in Al_2O_3.

5.5.2 Fe_2O_3 vs SiO_2 and Fe_2O_3 vs Al_2O_3 in the middle iron crust

The x-coefficient of the regression line of Fe_2O_3% versus Al_2O_3%

of samples 21, 23, 26, 27, 28, 29 and 30 is -3.25 and the x-coefficient of Fe_2O_3% versus SiO_2% -1.50. This indicates that a loss in total weight between sample 21 and 29 resulted in an increase in the TiO_2%.
Both graphs show that this loss is the result of leaching of Al_2O_3 and SiO_2. Because both graphs have a negative x-coefficient the x-coefficient is a measure to compare the degree in leaching of Al_2O_3 and SiO_2. Both x-coefficients suggest more severe leaching of SiO_2 than Al_2O_3. A change in Fe_2O_3 with 1 results into a change in SiO_2% of 1/-1.5 and Al_2O_3 of 1/-3.25.

5.5.3 Fe_2O_3 vs SiO_2 and Fe_2O_3 vs Al_2O_3 in the mottled zone of the middle iron crust

The x-coefficient of the regression line of Fe_2O_3% versus Al_2O_3% of samples 8, 10, 13, 14, 16, 17, 18, 19, 20, 21, 22, 24 and 25 is 0.51 and the x-coefficient of the regression line of Fe_2O_3% versus SiO_2% -0.338, indicating an increase in Al_2O_3 and a decrease in SiO_2 when Fe_2O_3 increases.
It is not possible to use x-coefficients as a measure to compare the degree of absolute leaching or accumulation. Negative and positive x-coefficients cannot be compared without a prior correction of the weight percentages for relative accumulation, due to loss in total weight.

5.6 CHEMICAL RESULTS OF THE HIGHESTS ELEVATED IRON CRUST

Samples 32, 33, 34, 35 and 36 were collected from the highest elevated iron crust in the research area. Chemical data of the four major elements (TiO_2, SiO_2, Al_2O_3 and Fe_2O_3) indicate absolute accumulation of Fe_2O_3 and leaching of SiO_2 and Al_2O_3. Leaching of SiO_2 seems more severe than leaching of Al_2O_3. The accumulation of Fe_2O_3 more than compensates for the loss in SiO_2 and Al_2O_3, resulting in a nett increase in total weight.
Calculation of the increase of Fe_2O_3 and the loss of SiO_2 and Al_2O3 assume no absolute accumulation or leaching of TiO_2.

Table 5.11: Weight percentages TiO_2, SiO_2, Al_2O_3 and Fe_2O_3 in sample 32 and sample 36.

	TiO_2%	SiO_2%	Al_2O_3%	Fe_2O_3%
Sample 36	1.81	14.79	15.78	67.47
Sample 32	2.41	30.29	25.15	42.32

TiO_2:
The accumulation of Fe_2O_3 and leaching of both SiO_2 and Al_2O_3 results in an increase of the total weight of 33.15% (equation 5.12).

$$\frac{2.41}{100+a} = \frac{1.81}{100} \qquad a = 33.15 \qquad (5.12)$$

Fe_2O_3:
The absolute accumulation of Fe_2O_3 resulted in an increase of the total weight with 47.52% (equation 5.13).

$$\frac{42.32+b}{133.15} = \frac{67.47}{100} \qquad b = 47.52 \qquad (5.13)$$

SiO_2:
The leaching of SiO_2 resulted in a decrease in total weight of 10.60% (equation 5.14).

$$\frac{30.29+c}{133.15} = \frac{14.79}{100} \qquad c = -10.60 \qquad (5.14)$$

Al_2O_3:
The leaching of Al2O3 resulted in a decrease of the total weight with 4.14% (equation 5.15).

$$\frac{25.15+d}{133.15} = \frac{15.78}{100} \qquad d = -4.14 \qquad (5.15)$$

Loss in SiO_2 and Al_2O_3 suggest ferralitization, ferrolysis and clay eluviation, next to absolute iron enrichment.
When the changes with regard to the granodiorite are calculated the succesive processes become more clear. The granodiorite contains 0.61% TiO_2, 63.21% SiO_2, 15.99% Al_2O_3 and 5.01% Fe_2O_3. Calculations were performed in the same manner as shown above, however the starting point was the granodiorite (constant TiO_2 % = 0.61).

Table 5.12: Loss or accumulation of SiO_2, Al_2O_3 and Fe_2O_3 (in weight percentages) in the samples 32 and 36 with regard to the parent material (sample 1).

	SiO_2	Al_2O_3	Fe_2O_3
sample 36	-58.23	-10.67	+17.73
sample 32	-55.54	-9.62	+5.70

When going up in the iron crust more SiO_2 and Al_2O_3 has leached (ferralitisation, clay eluviation and ferrolysis more severe). Furthermore more iron accumulates when going up in the profile. The possible origine of this iron will be discussed below. Figure 5.7 shows the three iron transport mechanisms which have been suggested by McFarlane (1976).

A LATERITE AS A RESIDUUM

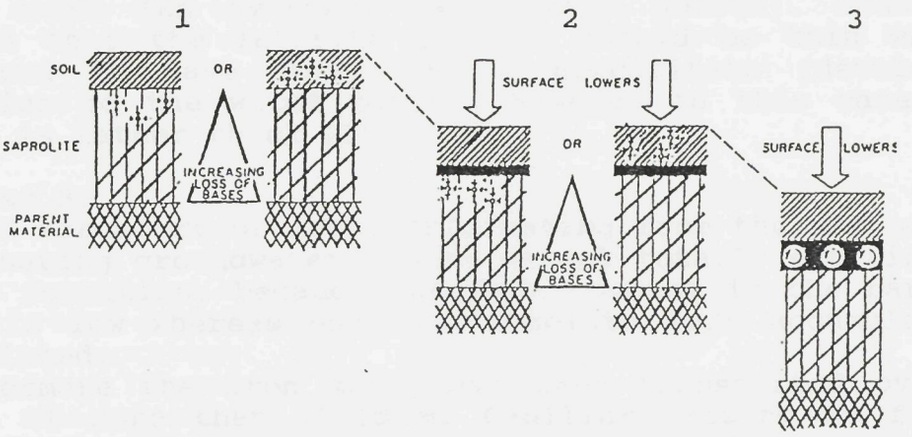

A downward process with an initial phase of limited mobility: precipitate formation (1); a phase of accumulation of relative immobile residuum (2) and a final phase of limited mobility: precipitates are altered under the influence of groundwater (3).

B LATERITE AS A PRECIPITATE

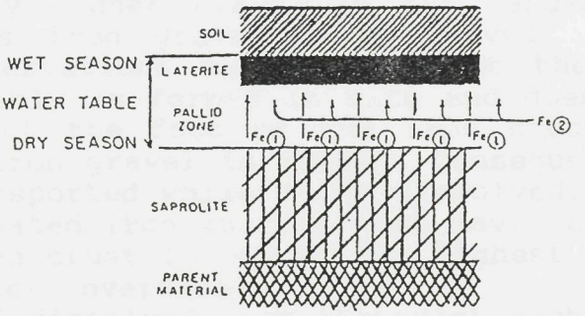

An upward process. Iron moves into the laterite in solution from the pallid zone (1) or a distant source (2)

C A DOWNWARD PROCESS FROM HIGHER LOCATIONS (LATERAL)

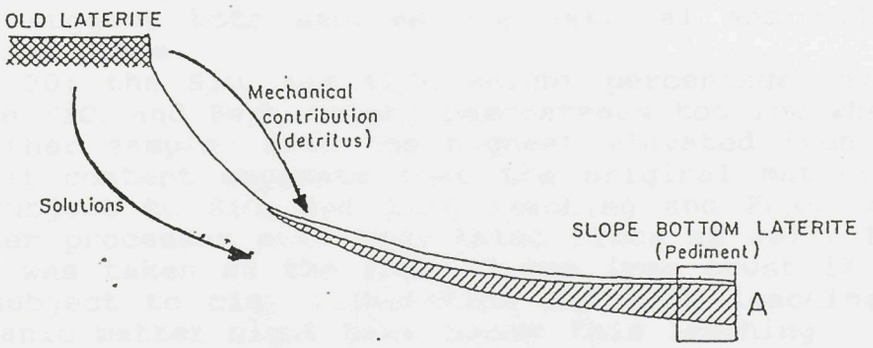

Figure 5.7: Three suggested processes of iron crust formation (after McFarlane, 1976).

Process A:
Iron might originate from the horizon originally overlying the iron crust (an overhead pedogenetic source). Goudie (1973) stated that the laterite horizon should be thin when it is supposed to have formed as a precipitate (development in relation to the water table). However in this case the iron crust is rather thick (10-15 m).

Process B:
Upward transport of iron, originating from the granodiorite by fluctuating groundwater tables cannot totally explain the iron crust formation, because the Fe_2O_3-content in the parent material is low whereas enormous absolute Fe_2O_3 accumulations are calculated.
Furthermore the iron must have been transported over a distance of more than 10-15 m. Capillary rising or fluctuating groundwater tables cannot explain transport over such a distance.

However both process A and B can partially explain the formation of the highest elevated iron crust. Furthermore a third mechanism of iron crust formation is suggested.

Process C:
The enormous iron accumulation suggest iron transport from topographically higher places in the landscape. Iron can be transported as iron gravel or dissolved. Micromorphological and field observations make clear that the highest elevated iron crust mainly is formed in situ and does not contain iron gravel (only at the foot of the iron crust, just below the surface, few iron gravel is found). Consequently the iron must have been transported while being dissolved. So topographically higher elevated iron sources must have been present. At the moment the iron crust is one of the highest elevated points in the area (relief inversion).
The process of dissolved iron transport might have been accompanied by the upward movement of iron at very small distances.

Samples 30 and 31 were also collected from the highest elevated iron crust. The two samples were collected from the second horizon of sampling site 6 at the foot of the iron crust. Chemical data of both samples show enormous differences with samples 32, 33, 34, 35 and 36 and among themselves. The differences suggest both samples are detrital and redistribution has taken place.
Sample 30: the SiO_2 and Al_2O_3 weight percentages are too high and the TiO_2 and Fe_2O_3 weight percentages too low when compared with other samples from the highest elevated iron crust. The chemical content suggests that the original material has not been subject to SiO_2 and Al_2O_3 leaching and Fe_2O_3 accumulation or other processes must have taken place as well. Because the sample was taken at the foot of the iron crust it might have been subject to clay illuviation and Fe_2O_3 leaching. Presence of organic matter might have caused this leaching.

Sample 31: the SiO_2% and Fe_2O_3% do not differ from the samples 32, 33, 34, 35 and 36. The Al_2O_3 is too low and the TiO_2 is too high. Assuming no absolute accumulation or loss of TiO_2 the high TiO_2% must have been caused by the loss of other elements. There seems to be an enormous loss in Al_2O_3. The origin of this loss is not known.

5.7 CHEMICAL RESULTS OF THE MIDDLE IRON CRUST

The samples 20, 21, 23, 24, 26, 27, 28, 29.
Assuming no absolute accumulation or leaching of TiO_2 the total weight has decreased causing a relative increase of the TiO_2 weight percentage. This slight decrease in total weight is thought to be caused by leaching e.g. of SiO_2 and Al_2O_3. However, the enormous increase of the Fe_2O_3 weight percentage cannot completely be explained by leaching of other elements. Absolute accumulation of iron also must have taken place because leaching of other elements would only result in an increase of the Fe_2O_3 to 17.32%.

Table 5.13: Weight percentages TiO_2, SiO_2, Al_2O_3 and Fe_2O_3 in sample 29 and sample 21.

	TiO_2%	SiO_2%	Al_2O_3%	Fe_2O_3%
Sample 29	1.50	44.79	24.79	28.61
Sample 21	1.36	57.69	30.54	9.52

As described above the slight increase of the TiO_2 percentage is thought to be caused by a slight decrease in total weight. An accumulation of Fe_2O_3 and leaching of SiO_2 and Al_2O_3 is thought to be the cause of the decrease in total weight. The total weight decreases to 100-9.33 = 90.67%.

TiO_2:

$$\frac{1.36}{100+a} = \frac{1.50}{100} \qquad a = -9.33\% \qquad (5.16)$$

Fe_2O_3:

$$\frac{9.52+b}{90.67} = \frac{28.61}{100} \qquad b = 16.42\% \qquad (5.17)$$

SiO_2:

$$\frac{57.69+c}{90.67} = \frac{44.79}{100} \qquad c = -17.08\% \qquad (5.18)$$

Al_2O_3:

$$\frac{30.54+d}{90.67} = \frac{24.79}{100} \qquad d = -8.06\% \qquad (5.19)$$

Loss is SiO_2 and Al_2O_3 indicates both ferralitization, clay eluviation and ferrolysis. Increase in Fe_2O_3 is caused by absolute iron enrichment.
Differences in SiO_2 (%), Al_2O_3 (%) and Fe_2O_3 (%) in the samples 21 and 29 with regard to the parent material are found in table 5.14.

Table 5.14: Loss or accumulation of SiO_2, Al_2O_3 and Fe_2O_3 (in weight percentages) in sample 21 and sample 29 with regard to the parent material (sample 1).

	SiO_2	Al_2O_3	Fe_2O_3
sample 29	-45.0	-5.91	6.62
sample 21	-37.34	-2.29	-0.74

The distance between sample 21 (363.50-364.00) and sample 29 (365.50-366.00) is about 2.5 m. This small distance (thin iron crust) could explain laterite formed as a residuum or laterite formed as a precipitate. As mentioned before, the granodiorite containes 0.61% TiO_2 and 5.01% Fe_2O_3. Assuming a constant TiO_2%, it becomes clear that upon weathering sampling point 21 showed an absolute loss in Fe_2O_3, although the relative amount Fe_2O_3 increased. The loss in iron could have been the result of an upward iron transport, which could also explain the absolute iron accumulation at sampling point 29.
The accumulation at sampling point 29 could however also be the result of a downward process originating from an overlying source or topographically higher sources. Whereas the loss found at sampling point 21 can be explained by a downward iron transport to the underlying pallid zone.
Again a third mechanism of transport of iron from adjacent areas might have been present. Micromorphological observations revealed transport of iron gravel but dissolved iron might also have been transported.
As the distances are not as large and the amount of iron transported not as big as found in the highest elevated iron crust, the contribution, of the overlying and underlying horizons to the Fe_2O_3 is probably bigger.

Sample 24 differs slightly from the other samples. The TiO_2 : Al_2O_3 ratio is in agreement with the ratio found in the other samples on the regression line. The SiO_2% however is too high and the Fe_2O_3% is too low, indicating a less severe accumulation of iron and less severe leaching of SiO_2.

The samples A, B, 38 and 39 consist of too low weight percentages of Al_2O_3 and TiO_2. The SiO_2% is too high and the Fe_2O_3% can be either too high or too low. When the TiO_2% is put in a graph against the SiO_2% or Fe_2O_3% the samples are located on the extention of the regression line. It is unknown why the samples occasionally are on the regression line of the other samples and occasionally differ. It must be noticed that the

samples 38, 39 and A and B are not taken from the middle crust.

5.8 CHEMICAL RESULTS OF THE MOTTLED ZONE OF THE MIDDLE IRON CRUST

The samples 5, 6, 7, 8, 9, 10, 11, 12, 13, 14, 15, 16, 17, 18, 19, 22 and 25.

Table 5.15: Weight percentages of SiO_2, TiO_2, Al_2O_3 and Fe_2O_3 in sample 17 and sample 8.

	SiO_2%	TiO_2%	Al_2O_3%	Fe_2O_3%
Sample 17	63.91	0.96	26.67	8.04
Sample 8	74.48	0.85	19.83	4.41

Between sample 8 and sample 17 the TiO_2% slightly increases indicating a minute decrease in total weight. As described before an absolute accumulation of Fe_2O_3 and Al_2O_3 and leaching of SiO_2 is supposed to have taken place.

TiO_2:

$$\frac{0.85}{100+a} = \frac{0.96}{100} \qquad a = -11.46 \qquad (5.20)$$

Fe_2O_3:

$$\frac{4.41+b}{88.54} = \frac{8.04}{100} \qquad b = 2.71 \qquad (5.21)$$

SiO_2:

$$\frac{74.48+c}{88.54} = \frac{63.91}{100} \qquad c = -17.89 \qquad (5.22)$$

Al_2O_3:

$$\frac{19.83+d}{88.54} = \frac{26.67}{100} \qquad d = 3.78 \qquad (5.23)$$

A decrease in total weight is caused by leaching of SiO_2 and absolute accumulation of Fe_2O_3 and Al_2O_3. Leaching of SiO_2 is explained by ferralitization. Increase in Fe_2O_3 is caused by absolute iron enrichment. Absolute Al_2O_3 enrichment is a nett result of accumulation by clay infilling and probably a SiO_2-loss by ferrolysis.

Table 5.16: Loss or accumulation of SiO_2, Al_2O_3 and Fe_2O_3 (in weight percentages) in sample 17 and sample 8 with regard to the parent material (sample 1).

	SiO_2	Al_2O_3	Fe_2O_3
sample 17	-22.60	+0.96	0.10
sample 8	-9.76	-1.76	-1.84

The absolute iron accumulation between sample 8 (altitude 361.37m) and 17 (362.54m) is small (2.7% see equation 5.21). Table 5.16 shows sample 8 has lost weight with regard to the parent material. The small distance (± 1.2m) combined with an accumulation of a small amount of iron and the loss of iron in sample 8 suggests the upward transport of iron (from sampling point 8 to 17). However accumulation from an overlying source (residuum) or transport from adjacent areas is also possible.

Samples 5, 6, 7, 11 and 12 differ from the other samples on the line regarding TiO_2 and Fe_2O_3 (too high) and SiO_2 and Al_2O_3 (too low). These samples might have been subject to more severe leaching of Al_2O_3 and SiO_2 and more severe accumulation of Fe_2O_3 compared with the overlying iron crust.

When comparing sample 7 with samples 5, 6, 11 and 12, small differences, attributed to differences in Al_2O_3%, are found. The Al_2O_3% of sample 7 is too low if compared with samples 5, 6, 11 and 12. This lower Al_2O_3% can be the result of a more severe leaching of Al_2O_3 or less severe clay illuviation.

6. CONCLUSIONS

In the research area three levels of iron crusts are present. Field and micromorphological observations show the largely in situ formation of the highest elevated and middle iron crust. The lowest iron crust is formed due to a combination of in situ formation and the deposition and cementation of iron gravel eroded from higher elevated iron crusts.
Field observations also show that the middle iron crust consists of two clearly separated layers. The lowest layer is the result of in situ formation. The highest layer consists of iron gravel inherited from higher altitudes.
At the foot of the highest iron crust also some detrital from higher altitudes is found.

Granodiorite is found at the surface in the research area. The granodiorite is thought to be the parent material which is confirmed by field- and micromorphological observations. Field observations display freshly weathered granodiorite at the sampling sites at the middle iron crust. Its presence is not shown, during field observations, at the highest elevated iron crust. This probably is the result of the severe iron impregnation, because micromorphological observation reveal the mineralogical composition of the original granodiorite and the saprolite in both middle and highest elevated iron crust are alike. The iron impregnation which is found at the highest iron crust, masks the presence of these freshly weathered granodiorite structures or mottles.

Micromorphological observations make clear that the presence of granodiorite is important for the formation of laterite in the research area, because clusters of iron-rich minerals are found in the parent material. These clusters act as cores around which iron mottles are formed. Upon hardening iron concretions are formed.

Chemical observations show that upon weathering the parent material first looses soluble oxides like MgO, Na_2O, K_2O, CaO, MnO and BaO. These soluble oxides are only found in the granodiorite and in the freshly weathered parent material.
When weathering proceeds a nett loss of SiO_2 is found. The hardly soluble SiO_2 will only leach during extremely wet periods when enormous amounts of water percolate through the soil.
Micromorphological observations show that this ferralitisation process is succeeded by the process of ferrolysis. Ferrolysis takes place under alternating wet and dry conditions. At the moment, in most of the samples, ferrolysis is a fossil process, because ferrolysis is not found in clay- or lime coatings, so must have preceeded these processes.

Ferrolysis is followed by iron accumulation. Furthermore clay coatings are found. Part of these coatings are subject to iron impregnation, so during and after iron accumulation and impregnation, clay illuviation took place.

The enormous iron accumulation which is found when going up in the highest elevated iron crust together with the thickness of this iron crust (>10m) indicates iron transport from adjacent areas. The underlying or overlying horizon can never totally explain this enormous iron accumulation. Iron can be transported from distant sources either as iron gravel or as dissolved iron. Since micromorphological and field observations suggest largely in situ formation (hardly any transported and cemented iron gravel), iron is probably dissolved and transported. Besides the above described mechanisms, the iron crusts may have been formed as a precipitate and/or a residuum.
The middle and lowest iron crusts are thinner and therefore it is possible to explain the iron accumulation in the crust to originate from overlying or underlying sources. Micromorphological observations however also display iron accumulation from adjacent areas, by transport of iron gravel.

The most recent process taking place in the iron crusts is the accumulation of lime, because it covers the clay coatings. Field observations show its very local presence, usually at the transition of white groundmass and iron mottles. Chemically a high lime is only found in the parent material, so the granodiorite is the source of the lime transport. Its presence is probably not shown in the other samples because only very locally lime concentrations were high, and the sample size reduced the locally high concentrations. Lime is transported either by termite activity, capillairy rising or both.

Assuming the TiO_2 to be homogeneously distributed in the parent material, the in situ formation of the iron crusts and assuming the TiO_2 to be chemically inert, the TiO_2-concentration should be constant in every sample. From this, absolute loss or accumulation of SiO_2, Al_2O_3 and Fe_2O_3, when going up in a profile, was calculated.
The extent of each process can not be calculated because several processes occur at the same time.

The graphs Al_2O_3 versus SiO_2, Fe_2O_3 versus Al_2O_3 and Fe_2O_3 versus SiO_2 reveal the relative age of each iron crust in the research area. Plotting data of samples of other iron crusts in the province of Sanmentenga could reveal the genesis of the landscape.

REFERENCES

Aleva, G.J.J. (compiler) and D. Creutzberg (editor), 1994, 'Laterites', Concepts, geology, morphology and chemistry, International Soil Reference and Information Centre, Wageningen.

Ambrosi, J.P. and D. Nahon, 1986, Petrological and geochemical differentiation of lateritic iron crust profiles, Chemical Geology: 57, p371-393.

Ambrosi, J.P., D. Nahon and A.J. Herbillon, 1986, The epigenetic replacement of kaolinite by hematite in laterite, Petrographic evidence and the mechanisms involved, Geoderma: 37, p289-294.

Bates, R.L. and J.A. Jackson, 1980, Glossary of Geology, 2nd edition, American Geol. Inst., Falls Church.

Brewer, R., 1964, Fabric and mineral analysis of soils, New York.

Brinkman, R., 1970, Ferrolysis, a hydromorphic soil forming process, Geoderma, 3: p199-206.

Brinkman, R., A.C. Jongmans, R. Miedema and P. Maaskant, 1973, Clay deposition in seasonally wet, acid soils: micromorphological, chemical and mineralogical evidence from individual argillans, Geoderma: 10, p250-270.

Brinkman, R., 1979, Ferrolysis, a soil-forming process in hydromorphic conditions, Wageningen.

Bullock, P., N. Fedoroff, A. Jongerius, G. Stoops and T. Tursina, 1985, Handbook for soil thin section description, Intern. Soc. of Soil Science, Wolverhampton.

De Swardt, A.M.J., 1964, Laterisation and landscape development in parts of equatorial Africa, Zeitsch. f. Geomorphologie, NF 8, p. 313-333.

Elkenbracht, E, A. ten Holte and L. Otter, 1994, Remote sensing and soil science of the Kaya area (Burkina Faso), Wageningen; Agricultural University (Antenne Sahélienne student report nr. 32).

FAO, 1990, Guidelines for soil description 3rd Edition (Revised), FAO, Rome.

Goudie, A., 1973, Duricrusts in tropical and subtropical landscapes, Oxford.

Grandin, G., 1976, Aplanissement cuirasses et enrichissement des gisement de manganese dans quelques regions d'Afrique de L'ouest, ORSTOM: no 82, Paris.

MacKenzie, W.S. and C. Guilford, Atlas of rock-forming minerals in thin section, Essex, 1980.

McFarlane, M.J., Laterite and Landscape, London, 1976.

Miedema,R., T. Pape and G.J. van der Waal, A method to impregnate wet soil samples, producing high-quality thin sections, Neth. J. Agric. Sci., 22: 37-39, 1974.

Munsell, 1975, Soil Color Charts, Baltimore.

ANNEX I: MAP BURKINA FASO

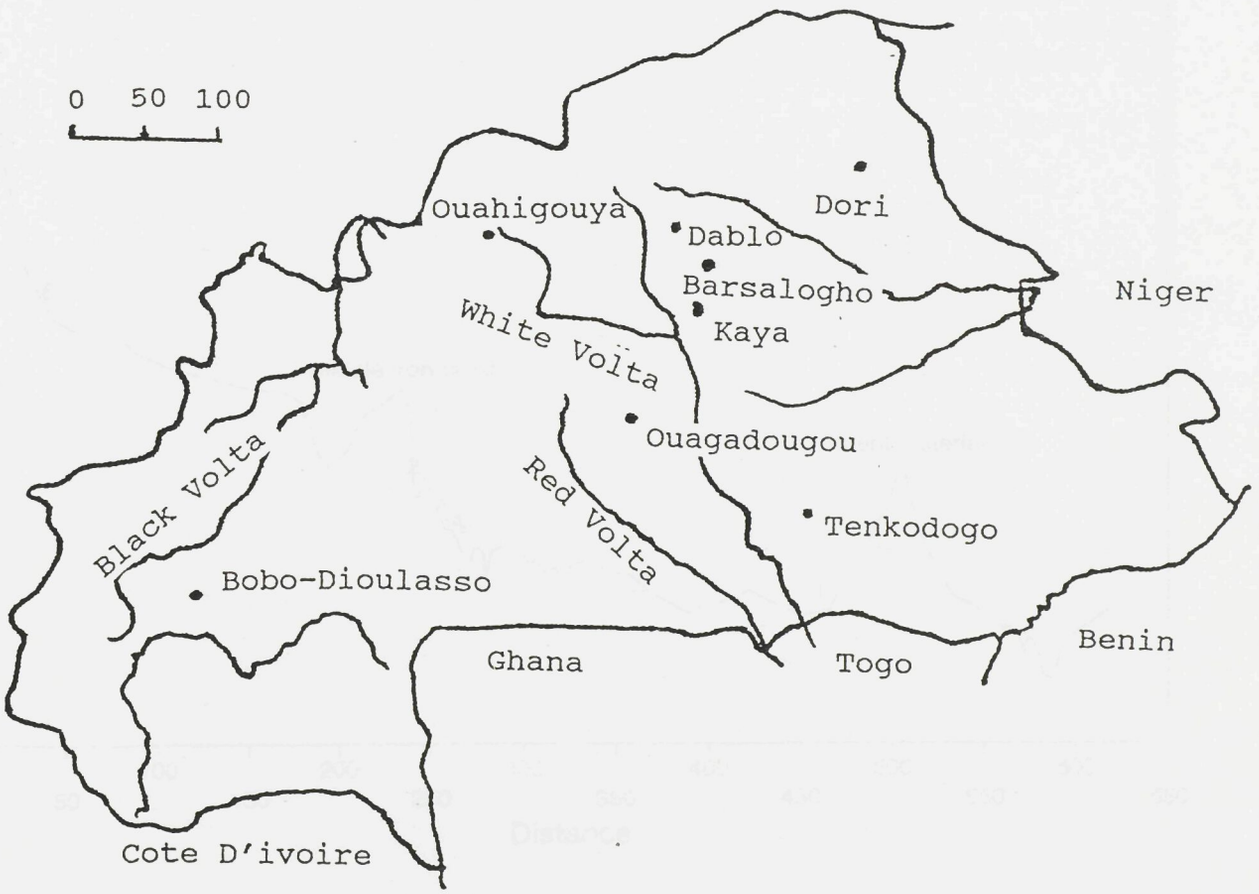

AN

385.00

highes

380.00

375.00

370.00

365.00

360.00

355.00

ANNEX II: CROSS-SECTION RESEARCH AREA

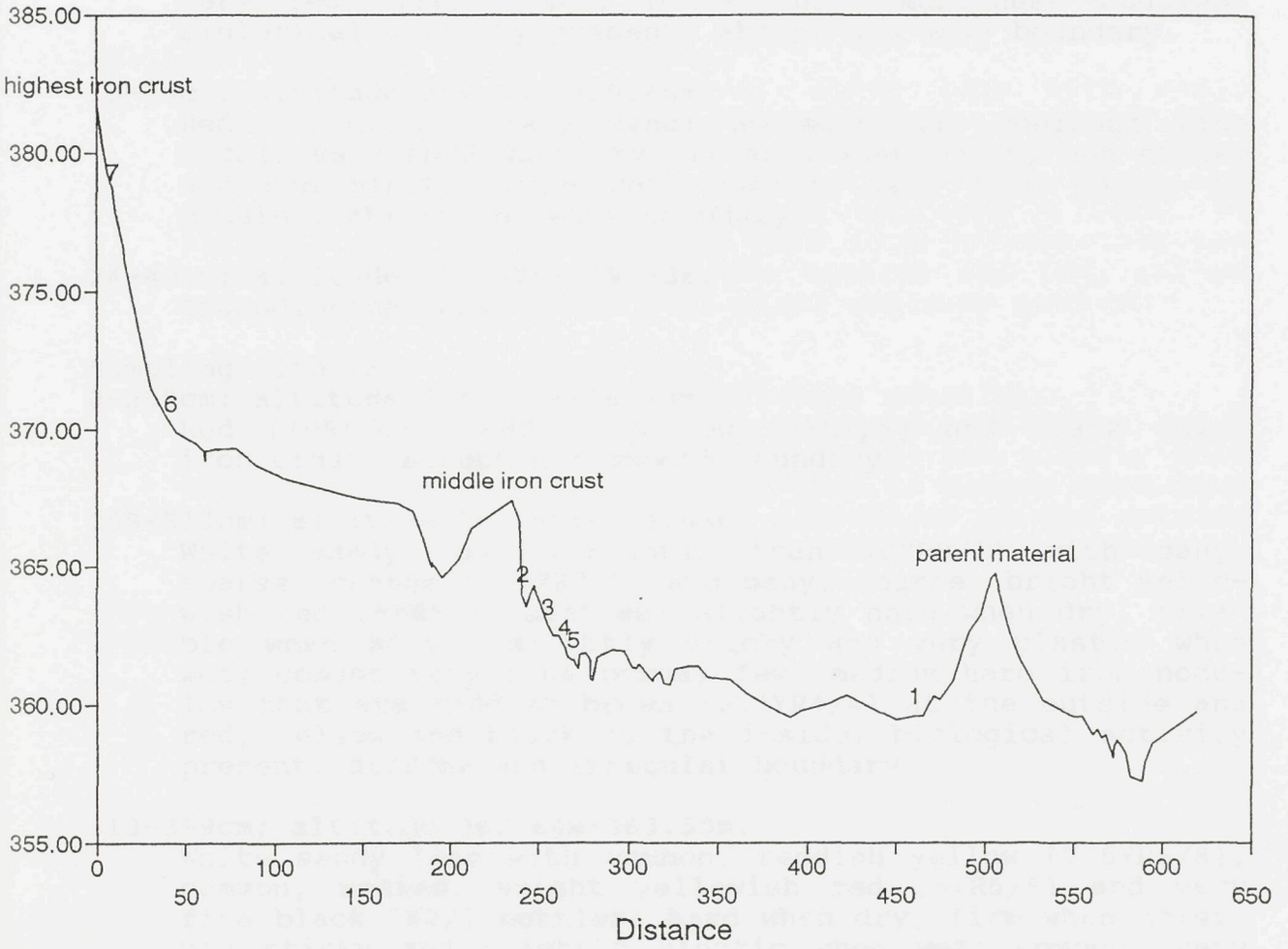

ANNEX III: SOIL PROFILE DESCRIPTIONS

Sampling site 1

0-15cm; altitude 359.66m-359.81m

Reddish yellow (7.5YR6/8) sandy loam; no mottling; very hard when dry, friable when moist, sticky and plastic when wet; few fine pores; abundant, medium to coarse, hard, iron nodules that are reddish brown (2.5 YR4/4) at the outside and red, yellow and black at the inside, and very few, fine, hard, black (N2/) manganese nodules; biological activity present; abrupt and wavy boundary.

15-24cm; altitude 359.58m-359.66m.

Red (2.5YR5/6) loamy sand; no mottling; dominant fine rocks; very hard when dry, friable when moist, non sticky and non plastic when wet; common, very fine pores; no nodules; abrupt and wavy boundary.

24-40cm; altitude 359.42m-359.58m.

Granodiorite rock.

Sampling site 2A

0-259cm; altitude 364.04m-366.63m.

Red (10R4/6), reddish yellow (5YR7/6) and black (N2/) iron crust; abrupt and smooth boundary.

259-313cm; altitude 363.50m-364.04m.

White sandy loam (brighter than 10YR8/1) with many, coarse, orange (2.5YR7/8) and many, coarse, bright yellowish red (5YR5/8) mottles; slightly hard when dry, friable when moist, slightly sticky and very plastic when wet; common very fine pores; few, medium hard iron nodules that are reddish brown (2.5YR4/4) at the outside and red, yellow and black at the inside; biological activity present; diffuse and irregular boundary.

313-399cm; altitude 362.64m-363.50m.

White sandy loam with common, reddish yellow (7.5YR6/8), common, medium, bright yellowish red (5YR5/8) and very fine black (N2/) mottles; hard when dry, firm when moist, non sticky and slightly plastic when wet; common, very fine pores; no nodules; biological activity present.

Sampling site 2B

0-43cm; altitude 363.09m-363.52m. Colluvium

Reddish yellow (5YR6/6) sandy loam; no mottling; very hard when dry; sticky and plastic when wet; many very fine pores; very few, medium, iron nodules that are reddish brown (2.5YR4/4) at the outside and red, yellow and black at the inside; abrupt and wavy boundary.

43-110cm; altitude 362.42m-363.09m.

White (brighter than 10YR8/1) sandy loam; abundant, very fine reddish yellow (5YR6/8) mottles; hard when dry, firm when moist, sticky and plastic when wet; very few, medium pores; common, medium, soft, iron nodules that are reddish brown (2.5YR4/4) at the outside and red, yellow and black at the inside.

ANNEX III: SOIL PROFILE DESCRIPTIONS

Sampling site 3A

0-25cm; altitude 362.54m-362.79m. Colluvium

Yellowish red (5YR5/6) sandy loam; no mottling; very hard when dry, firm when moist, slightly sticky and very plastic when wet; many very fine pores and very few fine pores; dominant, fine to medium, hard, iron nodules that are reddish brown (2.5YR4/4) at the outside and red, yellow and black at the inside; abrupt and wavy boundary.

25-120cm; altitude 361.59m-362.54m.

White (brighter than 10YR8/1) sandy loam with many, brownish yellow (10YR6/8) and common strong brown (7.5YR-5/6) mottles; hard when dry, firm when moist, slightly sticky and plastic when wet; common, very fine pores and very few, fine pores; between 96 and 98cm a layer of slightly flat and subangular, hard iron nodules that are reddish brown (2.5YR4/4) at the outside and red, yellow and black at the inside; biological activity present.

Sampling site 3B.

0-9cm; altitude 362.39m-362.48m. Colluvial material.

Reddish yellow (7.5YR6/6) sandy loam; no mottling; slightly hard when dry, slightly sticky and plastic when wet; many very fine pores; many fine to medium hard iron nodules that are reddish brown (2.5YR4/4) at the outside and red, yellow and black at the inside; abrupt and wavy boundary.

9-35cm; altitude 362.13m-362.39m.

White (brighter than 10YR8/1) sandy clay loam; many, fine, yellow (10YR7/8) and very few, very fine, yellowish red (5YR5/8) mottles; very hard when dry, slightly sticky and very plastic when wet; common very fine pores; no nodules; biological activity present; diffuse and wavy boundary.

35-80cm; altitude 361.68m-362.13m.

White (brighter than 10YR8/1) sandy clay loam with many very fine, yellow (10YR7/8) and yellowish red (5YR5/8) mottles; very hard when dry, slightly sticky and very plastic when wet; few very, fine pores; common, fine to medium, hard iron nodules that are reddish brown (2.5YR4-/4) at the outside and red, yellow and black at the inside; biological activity present; clear and wavy boundary.

80-100cm; altitude 361.48m-361.68m.

White (brighter than 10YR8/1) sandy clay loam with many, fine, yellow (10YR7/8) and very few, very fine, yellowish red (5YR5/8) mottles; very hard when dry, slightly sticky and very plastic when wet; few, very fine pores; no nodules.

ANNEX III: SOIL PROFILE DESCRIPTIONS

Sampling site 4.

0-65cm; altitude 361.84m-362.49m.

White (brighter than 10YR8/1) sandy clay loam with common, medium, red (2.5YR5/8) mottles; very hard when dry, sticky and very plastic when wet; common, very fine pores; very few, fine, hard iron nodules that are reddish brown (2.5YR4/4) at the outside and red, yellow and black at the inside; biological activity present; diffuse and wavy boundary.

65-79cm; altitude 361.70m-361.84m.

White (brighter than 10YR8/1) sandy clay loam with very few, medium, red (2.5YR5/8) mottles; very hard when dry, sticky and very plastic when wet; few, fine pores; common to many, medium, hard iron nodules; very few, fine iron nodules that are reddish brown (2.5YR4/4) at the outside and red, yellow and black at the inside; gradual and smooth boundary.

79-120cm; altitude 361.29m-361.70m.

White (brighter than 10YR8/1) sandy clay loam with common, coarse, red (2.5YR5/8) and yellow (10YR8/8) mottles; hard when dry, slightly sticky and very plastic when wet; common, very fine pores; very few, fine iron nodules that are reddish brown (2.5YR4/4) at the outside and red, yellow and black at the inside.

Sampling site 5

0-13cm; altitude 361.46m-361.59m.

Reddish yellow (5YR6/8) loamy sand; no mottling; soft to slightly hard when dry, slightly sticky and slightly plastic when wet; many, very fine pores and very few, fine pores; abundant, medium, hard iron nodules that are reddish brown (2.5YR4/4) at the outside and red, yellow and black at the inside; abrupt and smooth boundary.

13-61cm; altitude 360.98m-361.46m.

Pink (7.5YR7/4) sandy loam; no mottling; hard when dry, slightly sticky and very plastic when wet; common, very fine pores and very few, fine pores; abundant, medium, hard, iron nodules that are reddish brown (2.5YR4/4) at the outside and red, yellow and black at the inside; gradual and smooth boundary.

61-100cm; altitude 360.59m-360.98m.

White (brighter than 10YR8/1) sandy loam with many, red (2.5YR5/8) and few, yellow (10YR8/8) mottles; slightly hard when dry, sticky and plastic when wet; very few, fine pores; very few, very fine, black (N2/) iron and manganese nodules.

ANNEX III: SOIL PROFILE DESCRIPTIONS

Sampling site 6.
0-74cm; altitude 369.76m-370.50m.
Yellowish red (5YR5/8) sandy loam; no mottling; very hard when dry, sticky and very plastic when wet; very few, fine to medium and many, fine pores; dominant, medium to coarse, iron nodules that are reddish brown (2.5YR4/4) at the outside and red, yellow and black at the inside; biological activity present; clear and wavy boundary.

74-110cm; altitude 369.40m-369.76m.
Yellowish red (5YR5/8) sandy loam; no mottling; very hard when dry, sticky and very plastic when wet; very few, fine to medium pores; common, medium, hard iron nodules that are reddish brown (2.5YR4/4) at the outside and red, yellow and black at the inside.

Sampling site 7.
0-230cm; altitude 378.58m-380.88m.
Red (10R4/6), reddish yellow (5YR6/6) and black (N2/) very hard, iron crust; abrupt and wavy boundary.

230-340cm; altitude 377.48m-378.58m.
Red (2.5YR4/8) clay; hard when dry, very firm when moist; few, medium pores; abundant, hard iron nodules that are reddish brown (2.5YR4/4) at the outside and red, yellow and black at the inside; diffuse and smooth boundary.

340-420cm; altitude 376.68m-377.48m.
Red (2.5YR4/8) clay; hard when dry and very firm when moist; few, medium pores; dominant, hard, iron nodules that are reddish brown (2.5YR4/4) at the outside and red, yellow and black at the inside.

ANNEX IV: INFORMATION ABOUT SAMPLING

no.	Site	altitude	thin section number	remark
1	1	359.57	95026	granodiorite
1*	1	359.62	95001	saprolite
1*	1	359.65	95027	saprolite
2/3	1	359.70	95036	saprolite (2) and coluvial material (3)
4		not exactly known	-	altitude lower than sample 5
5	5	360.80	95035	deepest diagnostic horizon
6	4B	361.17	95033	first diagnostic horizon
7	5A	361.23	95031	2nd diagnostic horizon: presence of concretions
8	4B	361.37	95034	first diagnostic horizon
9	3B	361.66	95021	
10	4A	361.69	95032	
11	3A	361.73	95018	granite weathering
12	3B	361.73	95020	
13	3A	361.83	95017	presence of iron concretions
14	3A	362.22	95016	
15	3B	362.24	95019	
16	2B	362.54-362.93	95023	granite weathering
17	2B	362.54-362.93	95022	same altitude and site as sample 16
18	2A	not exactly known	-	infilling of a wormcast
19	2A	363.81	95006	
20	2A	not exactly known	-	iron from hydromorphic feature
21	2A	not exactly known	-	infilling of a root cast
	2A	363.50-364.00	95007	next to granite weathering
22	2A	363.50-364.00	95008	granite weathering
23	2A	364.30-365.00	95003	lowest layer of the middle iron crust
24	-	not exactly known	-	lowest layer of the middle iron crust

ANNEX IV: INFORMATION ABOUT SAMPLING

25		not exactly known	-	lowest layer of the middle iron crust
26		not exactly known	-	middle iron crust; (organic matter)
27		not exactly known	-	middle iron crust; (organic matter)
28		not exactly known		middle crust; (organic matter)
29		not exactly known		middle crust; (organic matter)
29*	2A	365.50-366.00	95002	highest layer of the middle iron crust
30	6	369.40-369.76	-	second diagnostic horizon
31	6	369.40-369.76	95040	second diagnostic horizon
32	6	369.76-370.50	95029	first diagnostic horizon
33	7	376.68-377.48	95015	third diagnostic horizon
34	7	377.48-378.58	95014	second diagnostic horizon
35	7	378.58-380.88	95013	first diagnostic horizon
36			95030	on top of the highest elevated iron crust
37			95037	under the lowest elevated iron crust
38		359.28	95038	the lowest elevated iron crust
39		359.28	95028	the lowest elevated iron crust
A		354.57	95042	laterite taken outside the research area
B		357.80	95041	laterite taken outside the research area
C		361.17	95043	laterite taken outside the research area
D			95039	laterite taken outside the research area

Samples

1-3 parent material and saprolite
4-29 middle one of the iron crusts
30-36 highest elevated iron crust
37-39 lowest elevated iron crust
A-D samples from laterite taken outside the research area

ANNEX V: THIN SECTION DESCRIPTIONS

The thin sections are described in the following order. At first the sampling sites 1 (granodiorite), 2, 3, 4 and 5 (the middle one of the iron crusts) are described, starting with the lower altitudes. As described in the results, the granodiorite is assumed to be the parent material but is not found at the sampling sites 2, 3, 4 and 5. The samples taken from the different sampling sites are alternated because altitudes are used to make a ranking. Sampling point and altitude are described.
Afterwards, samples taken from the highest and lowest iron crusts are described. Field observations suggested presence of chalc in some samples. Finally descriptions of thin sections consisting of chalc are found.
No chemical analysis are made from the samples accompanied by *.

Parent material and the middle one of the iron crusts.

Sample 1; thin section number 95026.
Sampling site 1; altitude 359.57m.

This granodiorite is thought to be the parent material. It was found just under the soil surface.
The following primary minerals are found: quartz, amfiboles (hornblendes), micas (sericite and a lot of biotite), feldspars (like microcline and anorthoclaas) and opaque iron-rich minerals. Iron-bearing minerals i.e. biotite, hornblende and opaque iron minerals, are found in a clustered distribution pattern.

Sample 1*; thin section number 95001.
Sampling site 1; altitude 359.62m.

This sample is taken from the horizon overlying the original granodiorite.
Again minerals like quartz, hornblende, biotite (and other micas), feldspars and opaque iron minerals are present.
Physical and mechanical weathering occur. The structure is dense but there is no isovolumetric weathering.
A dotted weathering is seen in alkali feldspares. The horn-2blendes demonstrate irregular alteration. Biotite shows a linear alteration and the weathering voids are partially filled with dark red iron compounds. The precence of a sharp knife-like weathering pattern of hornblendes suggests in situ weathering. The quartz minerals are hardly affected.
Iron-bearing minerals are found in a clustered distribution pattern. Vughs and channels are present. Coatings of dusty clay (40-50 μm) are found along the vughs and channels and minerals.

ANNEX V: THIN SECTION DESCRIPTIONS

Sample 1*; thin section number 95027.
Sampling site 1; altitude 359.65

This sample is also taken from the material overlying the granodiorite. See thin description sample 1*, thin section number 95001.

Sample 3; thin section number 95036.
Sampling site 1; altitude 359.70m.

This sample is taken at the transition from the weathered granodiorite to the colluvial material overlying the weathered material. This thin section seems only to consist of colluvial material. There are rounded minerals (weathered quartz, plagioclases and biotites) which are distributated homogeneously in a soil material. Suggesting the material has been transported. An iron nodule is also present. There is an abrupt transition from iron nodule to the groundmass, also suggesting the nodule has not been formed in situ.
It is assumed that this material has not been formed as a result of in situ weathering of the parent material (granodiorite).

Sample 5; thin section number 95035.
Sampling site 5; altitude 360.80m.

In this thin section 2 saprolites are present.
i A white saprolite. The fine material consists of clay booklets. These booklets look like kaolinite booklets which is confirmed by mineralogical analyses. The clayey material is probably arosen from weathering of alkali feldspars.
In the clayey material linear weathered and ironed biotites and strongly weathered hornblendes are found. Quartz minerals are cracked and fall apart into smaller parts. In the white saprolite pale yellow impure clay coatings are found.
ii Yellow saprolite. Micromorphological observations demonstrate that the yellow saprolite is built up exactly like the white saprolite. The difference is the randomly impregnation of iron in the yellow saprolite and the presence of pale yellow clay coatings in the white saprolite.
In this thin section the white saprolite is predominantly present. The yellow saprolite is especcialy found together with clusters of iron-bearing minerals.
The yellow saprolite is limpid, the white saprolite is grainy, and reflects bluish in incident light. In the white saprolite pale yellow dusty clay coatings are found, which are also reflecting blue in incident light. This proces has been described in Brinkman (1970 and 1979) and Brinkman *et al.* (1973) and is called ferrolysis. In the following thin sections the above describe observations are called ferrolysis.
Because the pale yellow coatings have become grainy these coatings must have been formed before the process of ferrolysis has started.
No limpid yellow coatings are found.

ANNEX V: THIN SECTION DESCRIPTIONS

Iron-bearing minerals are found in a clustered distribution pattern. Biotites weather and are filled with iron. The formation of amorphous iron nodules is starting at the iron-bearing minerals.
Secondary chalc is absent.

Sample 6; thin section number 95033.
Sampling site 4B; altitude 361.17m.

A large part of the thin section consists of white saprolite but occasionally yellow saprolite with large amounts of biotite occur. Both saprolites are found next to each other. No isovolumetric weathering. The white saprolite is grainy and impure pale yellow clay coatings are found. Both saprolite and coatings are subject to the process of ferrolysis. The process of the formation of iron-rich nodules has started but is not fulfilled.
Absence of red coatings and limpid yellow clay coatings.

Sample 7; thin section number 95031.
Sampling site 5A; altitude 361.23m.

The thin section consists of white saprolite and a lot of iron-rich nodules. Furthermore traces of yellow saprolite are present.
The white saprolite is subject to ferrolysis. A lot of large minerals are present. Yellow clay coatings are found accompanied by impure clay coatings, demonstrating absence of ferrolysis. The yellow coatings are not subject to ferrolysis as well. Ferrolysis is not an ongoing proces at this depth.
In the yellow saprolite, red coatings are found, which are locally covered with impure yellow coatings suggesting the latter are younger. In situ yellow coatings are also found.

Sample 8; thin section number 95034.
Sampling site 4B; altitude 361.37m.

Dominantly white and traces of yellow saprolite are present. Although the amount of yellow saprolite seems to increase when compared with the thin sections described before. In the white saprolite few pieces (papules) of pale yellowish impure clay coatings are found. Both features are subject to ferrolysis.
Few secondary chalc is found.
An iron nodule is found and it seems that more nodules are being formed by the process as described above.
Red clay coatings are absent.

Sample 9; thin section number 95021.
Sampling site 3B; altitude 361.66m.

The white saprolite and the yellow saprolite are present in almost the same amounts. Furthermore a brown-red material,

with a different b-fabric is present, although it accounts for only a small part of the thin section. The material consists especially of clay, fine quartz (50-60μm) and broken red clay coatings (papules). Concentration of biotite and fine material has taken place. Furthermore some organic matter is present. The microstructure is granular with compound packing voids and vughs as dominant voids. It is assumed that the brown-red material is formed by means of termite activity, and in following thin section descriptions it will be called termite material. Together with the termite material, secondary chalc is found along pores and in the groundmass. Termites might concentrate secondary chalc, but the accumulation of chalc can also be the result of cappilairy rising.
In the white material again in situ and fragmented (papules) pale yellow coatings are present. Both pale yellow coatings and the white saprolite are subject to ferrolysis so coatings must have been present before the process of ferrolysis started. Thin red clay coatings are also found in the white material, locally overlying the pale yellow coatings. They are limpid suggesting that ferrolysis is a fossil process at this depth, because the process did not affect them.
In the yellow saprolite also yellow coatings are found.

Sample 10; thin section number 95032.
Sampling site 4A; altitude 361.69m.

The thin section consist dominantly of white saprolite and traces of yellow saprolite are present. Iron-rich nodules and pale yellow coatings (in situ as well as fragmented) are found. The pale yellow coatings as well as the white saprolite groundmass are grainy, suggesting both are subject to ferrolysis. The pale yellow coatings must have been formed before the process of ferrolysis has started.
Biological activity is locally present (stritubules formed by termite activity). Both in the termite groundmass and along the termite material secondary chalc is found, concentrated by termite activity or by capillairy rising.
Iron-bearing minerals are found in a clustered distribution pattern. Iron seems to concentrate at these iron-rich minerals. The iron-rich areas increase and flow together (sometimes around the mineral still present). In this thin section a red nodule is formed around a quartz mineral.
In situ limpid red and yellow clay coatings are not observed.

Sample 11; thin section number 95018.
sampling site 3A; altitude 361.73m.

White saprolite dominates but yellow saprolite is also present. The white saprolite is grainy and therefore suggested to be subject to ferrolysis. Evidence of the presence of ferrolysis is also found in the in situ pale yellow clay coatings.
In the white saprolite also limpid yellow clay coatings are locally present and they are not subject to ferrolysis. They must have been formed after the process of ferrolysis has

stopped. This means ferrolysis is a fossil process at this depth.
Similar striotubules as found in 95032 are present.
Small iron nodules are present and nodules are also formed.
Presence of secondary chalc.

Sample 12; thin section number 95020.
Sampling site 3B; altitude 361.73m.

A white saprolite and yellow saprolite are present. Both saprolites are found next to each other, without a separation by coatings. There is slightly more white saprolite than yellow saprolite. Furthermore termite activity is seen. In the termite material secondary chalc is found, suggesting concentration of chalc by termites. A lot of secondary chalc also found along pores and in the white saprolite suggesting cappilairy rising.
Pale yellow coatings in situ as well as fragmented (papules) are found in the white material. The pale yellow coatings and the white saprolite are subject to ferrolysis. In the white saprolite also limpid yellow coatings are found, which are not subject to ferrolysis. The coatings must have been formed after the process of ferrolysis has ended suggesting ferrolysis is a fossil process at this depth.
The yellow material is occasionally coarse. Limpid yellow clay coatings are present in the yellow saprolite.
Again iron-rich nodules are found.

Sample 13; thin section number 95017.
Sampling point 3A; altitude 361.83m.

Predominantly termite material is present, but traces of yellow and white saprolite are also found. In the yellow and white saprolite limpid yellow clay coatings (in situ) are present. In some occasions the yellow clay coatings are covered with chalc. Absence of limpid red in situ coatings.
Termites seem concentrate fine material and probably secondary chalc. The microstructure is granular and it consists of compound packing voids and vughs.
Absence of in situ clay coatings in the termite material in contradistinction to the biological material in sample 14 (thin section number 95016). It suggests that biological activity was still present after the formation of limid red and limpid yellow coatings had stopped.

Sample 14; thin section number 95016.
Sampling site 3A; altitude 362.22m.

Both white and yellow saprolite are found. The yellow saprolite is much more fine than the white saprolite. In the yellow saprolite biological activity (striotubules) is present and could explain why this material is much more fine.
In the white saprolite (white coatings) as well as in the

yellow saprolite (yellow coatings) in situ claycoatings are present suggesting biological activity has happened before the precipitation of clay.
In some occasions white (pallish) coatings overlay the yellow clay coatings. That doesn't appeal to the theory because that means they are younger.
In the white saprolite locally ferrolysis is found. The pale yellowish coatings are present but are much more white than usual.
The red pappules are not present in the yellow saprolite.
Furthermore there are dusty yellow clay coatings.
Absence of secondary chalc.

Sample 15; thin section number 95019.
Sampling site 3B; altitude 362.24m.

Termite activity is alternated with the white saprolite. In both materials secondary chalc is found. It suggests chalc accumulation due to termite activity and capillairy rising.
In the termite material, in situ some impure clay coatings are found.
In the white saprolite limpid, yellow coatings as well as impure pale yellow coatings are present. The pale yellow coatings as well as the white saprolite groundmass are subject to ferrolysis. Because the coatings have a grainy appearance they must have been formed before the process of ferrolysis has started.
Red clay coatings are absent.
The transition between iron nodules and white saprolite is sharp suggesting no in situ formation of the nodules.

Sample 16; thin section number 95023.
Sampling site 2B; altitude 362.54-362.93m.

Presence of white saprolite, few yellow saprolite and few termite material.
The biotites in the white saprolite are impregnated with iron but the process of formation of iron nodules is less pronounced as seen in 95022.
Red clay coatings are found and yellow clay coatings can overly the latter.
Ferrolysis again is found in the white saprolite but not extreme.
Secondary chalc is observed.

Sample 17; thin section number 95022.
Sampling site 2B; altitude 362.54-362.93m.

The thin section consists mostly of white saprolite and termite material and very few yellow saprolite. A lot of iron filled clay pseudomophs often biotite is present.
Iron nodules, having diffuse transitions to the groundmass, are formed is situ.

ANNEX V: THIN SECTION DESCRIPTIONS

In the white saprolite red clay coatings (in situ) are found. Yellow clay coatings occasionally overly the red coatings. Secondary chalc is found especially along pores but also in iron nodules. This chalc might have been concentrated by capillairy rising and/or termite activity.
Ferrolysis seems to be present although not extreme.
Micromorphological observations of sample 17 and saple 16 make clear that both thin section resemble but differ in the amount of termite material and development of iron nodules.

Sample 19; thin section number 95006.
Sampling site 2A; altitude 363.81m.

Both yellow and white saprolite are present. Furthermore a red clayey material is present. In this material small rounded homogeneously distributed quartz minerals are found and fragmented red clay coatings (red papules).
In the white material pale yellowish papules are found. These papules are grainy. It is assumed that these pale yellow clay coatings which are found in the white material are similar to the red clay coatings present in the red material. The yellow material is probably excluded from the formation of these claycoatings due to preferent waterways.
Afterwards the structure collapsed and the coatings in the white material were exposed to the process of ferrolysis and became grainy. Both white saprolite and pale yellow coatings were subject to ferrolysis.
Traces of ferrolysis in the yellow and the red material are absent.
The red material is situated along the yellow material.
In the red material, yellow and white saprolite and between those three materials red clay coatings are present. These red coatings can be covered with yellow clay coatings. Both coatingstypes must have been deposited after the structure collapsed and also after the process of ferrolysis has ended because they are formed in situ and are not grainy.
The material does not display isovolumetric weathering.

Sample 21*; thin section number 95007.
Sampling site 2A; altitude 363.50m-364.00m.

The yellow and white saprolite are present. The saprolite is accompanied by the red material as described in sample 19.
Termite material is also found.
Furthermore this thin section consists of secondary chalc.
Secondary chalc is found in the saprolite and termite material. Suggesting the concentration by termites as well as capillairy rising.
It seems that the structure has been altered by termite activity. The secondary chalc is also attacked by termites. It is speculated that termites select certain parts of the saprolite (especially small quartz grains and small papules) and chalc.
Furthermore iron-bearing minerals are found in a clustered

distribution pattern and impregnated with iron. Iron nodules are starting to form.

Sample 22; thin section number 95008.
Sampling site 2A; altitude 363.50m-364.00m.

The yellow and white saprolite are observed. Termite material is also present. In the saprolite aggregates with soil are found as impurities.
Although ferrolysis is taken place in the white saprolite it is not extreme, as shown in its grainy appearance.
Red iron nodules are starting to form. Although this sample is found at the same altitude as sample 21* at the same sampling site, both samples differ substantially. In this thin section red material as described above is absent.
Red clay coatings are found. Yellow clay coatings can overly the red coatings. Both yellow and red coatings are weak grainy.

Sample 23; thin section number 95003.
Sampling site 2A; altitude 364.30m-365.00m.

The middle ironcrust consists of two clearly separated layers. This sample is taken from the lower part.
This lower part seems to differ from the upper part of the ironcrust.
There are two different groundmasses:
A yellow material consisting of clay booklets.
A red groundmass with very few small quartz minerals.
Iron filling (in matrix) has taken place and iron coatings are present. Furthermore fragmented red and yellow clay coatings (pappules) are found.
In the red material as well as in the yellow material and between both material red clay coatings are found. The coating can be covered with yellow claycoatings suggesting the latter is formed after the red coatings were present.
Micromorphological observations suggest the original structure consisting of a red groundmass overlying a yellow material collapsed. After the structure collapsed clay coatins were formed.

Sample 29*; thin section number 95002.
Sampling site 2A; altitude 365.50m-366.00m.

The middle one of the ironcrusts consists of two clearly separated layers. This sample represents the upper part of the middle one of the iron crusts.
Rounded aggregates of especially yellow saprolite but also of white saprolite. The yellow and white saprolite seem to consist of claybooklets. In the yellow saprolite areas heavily impregnated with iron are found. Occasionally the iron impregnated areas consist of angular cavities. Quartz grains seem to have disappeared from the cavities.

ANNEX V: THIN SECTION DESCRIPTIONS

Along the aggregates layers of pure iron are found. The presence of rounded aggregates suggests it is detrital from higher altitudes.

The highest elevated iron crust

Sample 31; thin section number 95040.
Sampling site 6; altitude 369.76m-370.50m.

The groundmass consists of:

i Dark red angular iron gravel (50μm-2cm) of alternating composition regarding primary minerals (amount of totally weathered partially ironed clay pseudomorphs after biotites and quartz grains). Occasionally quartz grains are totally weathered and have disappeared. An iron framework remains.

ii A heterogeneous material consisting of aggregates. A yellow-red material with clay infillings and big quartz minerals (300μm). In the small aggregates iron gravel is found. Furthermore layers of pure iron with strong birefringe are found suggesting a continuous support of iron.

Both the heterogeneous internal fabric between the nodules and the angular broken nodules itself, suggest that the material found in this thin section is detrital. The different materials are impregnated and cemented by iron.

Sample 32; thin section number 95029.
Sampling site 6; altitude 369.40m-369.76m.

This thin section consists of an iron nodule. Nodules are commonly found in the diagnostic horizon. The nodules displays the presence of many angular cavities in which quartz minerals can be present. The quartz minerals are usually smaller than the cavities. This is probably not the result of thin section preparation because the surface of the quarz minerals is usually smooth. It seems that the quartz minerals are starting to weather. Occasionally the quartz minerals have totally disappeared and a framework of iron remains. Locally the cavities are filled with clayey material. Occasionally pieces of quartz minerals are found in the clayey material.
Furthermore small (20-500μm) white sperical to elipsocal aggregates are present. The aggregates consist of small (50 μm) quartz minerals and a grainy white clayey material. The white clayey material reflects blue when incident light is used. It is subject to ferrolysis.
The aggregates are surrounded by dark red iron and within the aggregates iron droplets, in alternating amounts, are found.
It is speculated that erosion material of white saprolite and quartz grains is cemented by iron. It is not known why the white saprolite has been deposited at this place. It might be detrital but the aggregates could also be the result of biological activity.

ANNEX V: THIN SECTION DESCRIPTIONS

Sample 33; thin section number 95015.
Sampling site 7; altitude 376.68m-377.48m.

i Dark red iron nodules, big (600-800 μm) quartz grains and totally weathered, clayed and iron impregnated clay pseudomorphs after biotites are observed. Weathering is isovolumetric.
Locally frameworks of iron are found. It it suggested that quartz grains which must have been present (angular cavities) have disappeared by weathering.

ii Aggregates of a light red clayey material consisting of clay booklets smaller sized than those found in the dark red nodules. Occasionally big quartz grains are found. There are less quartz grains and the quartz grains are smaller than those found in the dark red iron nodules.
In the intergranular cavities limpid to impure caly coatings are found. The majority of the coatings found are formed in situ.

Both material have the same mineralogical composition (quartz grains and micas). Between both material sharp boundaries are found.

Sample 34; thin section number 95014.
Sampling site 7; altitude 377.48m-378.58m.

i Dark red saprolite with big quartz grains (600-700μm), clay pseudomorphs after micas and ironed hornblendes are present. Internal fabric in terms of presence of partially isovolumetric weathering are observed suggesting this is the saprolite. The saprolite has been heavily impregnated with iron
Along the surface of the nodule a grey clayey material which seems to have been unironed is present without an isovolumetric saprolite structure.

ii Light red clayey material with a granular microstructure suggesting biological activity. No iso-volumetric weathering. Locally big quartz grains are found. Presence of small kaolinite booklets. Orange red dusty clay fillings. Compound packing voids and vughs.

Dark red saprolite and light red clayey material have the same mineralogical composition. It is speculated that both materials have the same origin. In the light red material weathering has been more strongly proceeded.

Sample 35; thin section number 95013.
Sampling site 7; altitude 378.58m-380.88m.

Two materials are present:

i A red/yellow material which consists mainly of iron and locally of clayey soil material. A booklet structure is found in this clayey material. Furthermore iron frameworks are found. Quartz grains seem to have disappeared which resulted

into the formation of angular cavities. No isovolumetric weathering structure is seen in this saprolite. The saprolite is not as red as the saprolite found in the underlying horizons.

ii Red soil material. Locally a granular microstructure is found and between the granules, clay infillings are present. The soil material is more red than the soil material found in the underlying horizons.

Sample 36; thin section number 95030.
Sampling point; on top of the highest ironcrust in the sampling area; altitude not exactly known.

Presence of yellow saprolite consisting of clay booklets and clay pseudomorphs after biotites. In the yellow saprolite locally red areas consisting of ironed saprolite are present. The red areas seem to have the same composition. Claybooklets are also present and no quartz grains are found. Micromorphological observations in terms of mineralogical composition suggest in situ formation of red areas of ironed saprolite. The yellow saprolite is locally heavily impregnated with iron.

The lowest elevated iron crust

Sample 37; thin section number 95037.
Sampling point; the lowest elevated iron crust; altitude not exactly known.

Three materials are observed:
i A white saprolite with a groundmass of fine, white grainy clay in a booklet structure. Pale yellow grainy clay coatings are observed suggesting that the pale yellow coatings as well as the white saprolite are subject to ferrolysis.
ii Ferric nodules. The ferric nodules consist of the same amount of quartz minerals as found in the white saprolite. Furthermore structures of clay booklets with weathered and ironed biotites and coarse quartz grains are found. Again the weathered biotites seems to form cores were iron is deposited. Micromorphological observations in terms of internal fabric suggest in situ formation of ferric nodules resulting in an in situ formation of the iron crust.
iii Iron gravel with a b-fabric differing from the ferric nodules and the white saprolite described above. The transition between iron gravel and the adjacent material is sharp. Regarding different b-fabric and sharp edges the iron gravel seems to be detrital supplying from higher altitudes.
Micromorphological observations suggest both in situ formation and inheritance of the lowest elevated iron crust.

ANNEX V: THIN SECTION DESCRIPTIONS

Sample 38; thin section number 95038.
Sampling point; the lowest elevated iron crust; altitude not exactly known.

Abundant iron compounds are found in this thin section. Two materials are distinguished.
i Aggregates of white saprolite consisting of grainy clay booklets and coarse (250μm) quartz grains. Presence of pale yellow grainy clay coatings. Both pale yellow coatings and white saprolite are subject to ferrolysis.
ii Aggregates of yellow saprolite with clay booklets and coarse quartz grains.
The aggregates are covered with iron coatings
Furthermore presence of in situ red and yellow saprolite.

Presence of both round aggregates consisting of saprolite and red and white saprolite suggests in situ formation as well as presence of detrital. In situ formation as well as inheritance of the lowest elevated iron crust is suggested.

Sample 39; thin section number 95028.
Sampling point; the lowest elevated iron crust; altitude not exactly known.

Two materials are distinguished
i A white saprolite consisting of grainy clay booklets, coarse quartz grains (200-500μm) and light yellow papules. Both saprolite and papules are subject to ferrolysis but not extreme. Furthermore presence of in situ impure pale yellow clay coatings.
ii Dark red ferric nodules consisting of clay booklets and weathered and ironed biotites. Presence of quartz grains up to 500-600μm.
The transition between the dark red ferric nodules and the white saprolite is sharp and covered with pure iron. The sharp transition suggests an inheritance of the ferric nodules.

Samples containing chalc

Sample 40*; thin section number 95009.
Sampling point soil surface; altitude not exactly known.

This material was found at the soil surface and is probably deposited at the surface when research was done last year.
This thin section consists mostly of secundary chalc, quartz and a few hornblende. Iron is visible along cracks. The original red material is seen next to the chalc. This chalc may be impregnated with iron. At a high pH the iron will deposit. Also chalced micas are found.
The weathering of the original rockstructure will take place at low pH-values. The presence of chalc will result in high pH-values. This means that at first the rock structure is weathered. During this period these minerals are kept in place

by e.g. clay. Later the clay and the weathered minerals must have been impregnated with chalc.

Sample 41*; thin section number 95010.
Sampling point soil surface; altitude not exactly known.

This material was found at the soil surface. It is assumed that this material is deposited at the soil surface by means of human activity.
A saprolite consisting of quartz and a fine groundmass of clayey material. Chalc is found impregnated in weathered quartz grains and feldspars. Clay infilling are observed along pores. These clay coatings are heavily impregnated with iron. On this red clay coatings, a yellow clay coating is visible. This layer is covered by a chalc coating.
Impregnation with chalc seems to succeed weathering of the original granodiorite. Weathering is fulfilled when the pH is low and the pH increases when chalc is present.

ANNEX VI: MINERALOGICAL RESULTS

	quartz	kaolinite	goethite	hematite	divers
1	+++	-	-	-	Pl:+++;Or:+;Am.:++;Mi:+
2	++	+/-	-	-	Or:+;Pl:+;Am:+;Ch:+
3	++++	+	+	-	Or:+;Pl:+;Am:+/-
4	+++	++	+	+	Or:+/-
5	+++	+++	+	+/-	
6	+++	+++	++	+	Or:+/-
7	+++	+++	+	+	Or:+/-
8	+++	+++	+	+/-	Or:+/-
9	+++	+++	+	+/-	
10	+++	+++	+	+/-	
11	+++	+++	+	-	
12	+++	+++	+	+	Or:+/-
13	+++	+++	+	-	Or:+/-
14	+++	+++	+/-	-	Or:+/-
15	+++	+++	-	-	Or:+/-;Pl:+/-;Sm:+/-
16	+++	+++	+	+	
17	+++	+++	+	+	
18	+++	+++	+/-	+/-	Or:+
19	+++	+++	+	+/-	
20	+++	+++	+	+/-	
21	+++	+++	+	+/-	
22	+++	+++	+	+/-	
23	+++	+++	+	+	
24	+++	+++	+	+/-	
25	+++	+++	+	+/-	
26	+++	+++	+	+	
27	+++	+++	+	+	
28	+++	+++	+	+	
29	+++	+++	+	+	
30	+++	+++	+	+	
31	++	+++	+++	+	
32	+	+++	++	++	
33	*	*	*	*	
34	*	*	*	*	
35	*	*	*	*	
36	+	++	+++	+	
37	+++	+++	+	+/-	Or:+
38	+++	+++	++	+	Or:+/-
39	+++	+	++	+	Or:+/-
A	+++	++	++	+	
B	+++	++	++	+	
C	+++	+++	++	+	
D	++	+++	++	++	

Relative Amount	
-	not present
+/-	very little or doubtfull
+	few
++	moderate
+++	much
++++	very much
*	no mineralogical analyses
Am	Amfibole
Ch	Chlorite
Mi	Mica
Or	Alkali-feldspar
Pl	Plagioclase
Sm	Smectite

ANNEX VIIA: CHEMICAL RESULTS: MAIN ELEMENTS

	SiO2	TiO2	Al2O3	Fe2O3	MnO	MgO	CaO	Na2O	K2O	P2O5	BaO
1	63.21	0.61	15.99	5.01	0.08	2.90	4.45	4.81	2.67	0.18	0.10
2	65.00	0.61	18.97	5.32	0.05	1.88	2.43	3.02	2.54	0.03	0.12
3	79.20	0.66	11.77	5.91	0.08	0.48	0.32	0.17	1.30	0.03	0.04
4	59.57	1.13	16.55	22.48	0.10	0.11	0.01	0.04	0.22	0.06	0.03
5	63.34	1.02	21.51	13.15	0.52	0.16	0.01	0.04	0.30	0.08	0.17
6	65.57	0.92	22.32	10.74	0.07	0.13	0.22	0.04	0.23	0.04	0.03
7	62.14	1.16	18.56	18.12	0.04	0.09	0.01	0.04	0.13	0.04	0.03
8	74.48	0.85	19.83	4.42	0.01	0.12	0.08	0.04	0.41	0.02	0.03
9	64.40	0.94	24.01	10.06	0.01	0.26	0.27	0.04	0.23	0.03	0.03
10	69.05	0.92	22.33	7.03	0.20	0.18	0.15	0.04	0.26	0.03	0.08
11	64.01	1.09	22.10	11.62	0.37	0.23	0.19	0.04	0.40	0.07	0.08
12	60.18	1.15	21.31	16.48	0.24	0.26	0.10	0.04	0.30	0.03	0.10
13	68.37	0.86	22.78	7.74	0.06	0.12	0.02	0.04	0.24	0.03	0.03
14	68.84	0.93	22.36	6.73	0.11	0.29	0.43	0.04	0.41	0.02	0.03
15	77.11	0.79	14.79	5.49	0.06	0.49	0.60	0.04	0.71	0.02	0.03
16	64.69	1.01	25.40	8.47	0.15	0.12	0.08	0.04	0.21	0.05	0.03
17	63.91	0.96	26.67	8.04	0.16	0.11	0.09	0.04	0.20	0.07	0.04
18	72.50	0.93	20.20	4.29	0.07	0.34	1.13	0.04	0.59	0.05	0.03
19	65.36	0.83	25.38	8.16	0.02	0.08	0.12	0.04	0.21	0.08	0.03
20	57.13	1.38	29.74	10.44	0.03	0.25	0.31	0.23	0.41	0.06	0.03
21	57.69	1.36	30.54	9.52	0.03	0.18	0.20	0.09	0.35	0.06	0.03
22	66.90	0.95	24.78	7.32	0.04	0.07	0.01	0.04	0.20	0.06	0.03
23	47.89	1.48	25.95	24.83	0.06	0.04	0.01	0.04	0.01	0.07	0.03
24	58.68	1.39	29.09	10.28	0.03	0.22	0.11	0.04	0.29	0.04	0.03
25	61.44	1.05	27.93	9.36	0.03	0.09	0.08	0.04	0.20	0.03	0.03
26	48.72	1.47	27.08	22.66	0.09	0.09	0.01	0.04	0.10	0.08	0.03
27	44.79	1.50	24.79	28.61	0.25	0.14	0.02	0.04	0.08	0.08	0.03
28	53.23	1.43	28.72	16.51	0.05	0.10	0.03	0.05	0.15	0.05	0.03
29	47.11	1.42	25.51	26.00	0.06	0.07	0.01	0.04	0.02	0.10	0.03
30	51.76	1.67	27.80	18.81	0.04	0.04	0.01	0.04	0.07	0.11	0.03
31	24.17	3.48	17.46	54.93	0.04	0.08	0.01	0.04	0.00	1.01	0.03
32	30.29	2.41	25.15	42.32	0.03	0.03	0.01	0.04	0.00	0.24	0.03
33	28.55	2.10	23.73	47.18	0.03	0.06	0.01	0.04	0.00	0.22	0.03
34	26.10	2.28	22.59	50.35	0.03	0.04	0.01	0.04	0.00	0.27	0.03
35	19.79	2.05	19.96	47.18	0.04	0.05	0.01	0.04	0.00	0.45	0.03
36	14.79	1.81	15.78	67.47	0.06	0.11	0.06	0.04	0.00	0.45	0.03
37	67.16	0.95	20.47	10.97	0.02	0.12	0.01	0.04	0.55	0.02	0.03
38	42.91	1.53	20.43	34.90	0.33	0.08	0.01	0.04	0.00	0.10	0.03
39	40.08	1.54	17.49	40.57	0.22	0.12	0.01	0.04	0.08	0.10	0.08
A	41.79	1.48	16.95	39.12	0.52	0.11	0.01	0.04	0.08	0.13	0.09
B	41.18	1.50	22.01	35.07	0.10	0.13	0.06	0.04	0.02	0.20	0.03
C	44.33	1.21	23.37	31.30	0.08	0.06	0.01	0.04	0.00	0.06	0.03
D	35.34	2.11	18.26	44.19	0.11	0.15	0.01	0.04	0.00	0.22	0.03

All expressed as weight percentage

ANNEX VIIB: CHEMICAL RESULTS: TRACE ELEMENTS

	Ba	Co	Cr	Cu	Ga	La	Nb
1	924.85	29.06	53.11	23.05	25.05	<	11.02
2	1212.15	14.47	52.70	55.80	29.97	<	13.43
3	571.16	15.78	61.01	38.92	22.09	<	25.24
4	479.52	27.95	379.53	56.98	27.95	37.63	22.58
5	1796.41	29.40	94.72	86.01	30.48	<	22.86
6	389.34	<	95.42	83.35	31.81	31.81	18.64
7	149.05	15.01	189.79	67.55	31.10	26.81	30.02
8	123.38	<	57.36	35.71	30.30	<	22.73
9	<	<	80.97	45.47	31.06	<	18.86
10	777.94	<	60.43	50.54	30.77	<	21.98
11	1022.83	150.35	113.04	93.28	32.92	<	18.66
12	1099.99	83.78	169.73	53.31	31.55	29.38	26.11
13	138.44	13.29	56.48	35.44	31.01	<	12.18
14	377.96	81.54	56.20	48.48	31.96	<	23.14
15	336.63	<	47.32	26.89	23.66	21.51	33.34
16	517.43	111.11	68.63	65.36	33.77	22.88	18.52
17	527.19	63.40	61.17	57.84	36.70	20.02	16.68
18	226.40	<	43.96	39.56	26.38	20.88	39.56
19	177.62	14.43	57.73	58.84	33.30	29.97	17.76
20	<	<	93.61	51.26	37.89	34.55	30.09
21	74.13	<	81.99	46.05	39.31	50.54	30.33
22	121.75	78.58	87.44	47.59	34.31	17.71	12.17
23	<	<	268.27	52.99	35.33	39.74	20.98
24	143.37	<	101.93	47.04	40.32	26.88	31.36
25	162.52	<	62.77	63.89	35.87	43.71	20.17
26	<	<	226.48	48.21	37.00	24.67	22.42
27	<	44.35	327.05	52.11	39.91	32.15	27.72
28	<	<	147.72	36.08	37.21	20.30	27.06
29	<	14.47	288.23	65.66	38.95	40.06	20.03
30	117.82	<	293.99	50.65	37.44	71.57	40.74
31	<	338.66	949.37	320.90	24.43	69.95	18.88
32	<	111.48	617.00	27.59	38.63	268.21	27.59
33	n.a.	n.a.	n.a.	n.a.	n.a.	n.a.	n.a.
34	n.a.	n.a.	n.a.	n.a.	n.a.	n.a.	n.a.
35	n.a.	n.a.	n.a.	n.a.	n.a.	n.a.	n.a.
36	<	588.96	534.20	284.98	21.23	<	<
37	166.41	<	96.80	51.12	28.28	<	19.58
38	613.12	84.61	461.49	38.46	29.67	<	24.17
39	1407.78	136.87	571.37	83.64	32.59	22.81	18.47
A	1337.64	134.53	498.74	49.22	29.53	17.50	24.06
B	597.05	105.75	413.09	90.33	31.95	<	24.23
C	<	50.96	320.15	40.99	31.02	<	23.26
D	<	182.51	1528.96	120.22	41.53	37.16	13.11

< lower than detection limiet

n.a. not analysed

All expressed in parts per million (ppm)

ANNEX VIIB: CHEMICAL RESULTS: TRACE ELEMENTS

	Ni	Pb	Rb	Sr	V	Zn	Zr
1	102.20	14.03	75.15	855.71	98.20	72.14	182.36
2	66.14	16.53	65.10	645.86	110.57	83.70	187.04
3	48.39	19.99	52.59	151.47	109.39	15.78	375.51
4	21.50	39.78	15.05	39.78	318.25	<	358.03
5	39.19	78.39	20.69	35.93	210.13	42.46	263.47
6	40.58	29.61	13.16	59.22	199.61	25.22	298.31
7	28.95	30.02	10.72	41.82	295.95	<	486.81
8	41.13	19.48	20.56	55.19	140.69	<	419.91
9	46.58	17.75	<	86.51	167.48	36.60	256.21
10	32.96	30.77	<	78.01	156.03	<	313.15
11	51.58	52.68	21.95	69.14	234.86	48.29	280.95
12	44.61	50.05	17.41	87.04	258.95	18.50	353.61
13	43.19	15.51	12.18	40.98	140.66	24.37	265.81
14	38.57	39.67	19.83	90.36	170.80	24.24	349.31
15	46.25	20.43	27.96	138.74	122.61	33.34	494.73
16	66.45	23.97	10.89	54.47	194.99	38.13	296.30
17	46.71	18.91	12.23	51.16	170.17	34.48	255.81
18	19.78	17.58	28.57	156.06	150.57	<	626.44
19	68.83	18.87	<	49.96	148.76	44.40	230.91
20	36.78	23.40	16.72	139.31	277.50	<	455.81
21	34.82	24.71	14.60	116.81	272.94	<	417.84
22	78.58	12.17	12.17	34.31	157.17	44.27	229.11
23	19.87	35.33	<	37.54	384.19	<	327.89
24	38.08	24.64	14.56	80.65	282.26	<	481.63
25	38.11	22.42	<	49.32	202.87	<	379.96
26	23.55	43.73	13.45	34.76	381.21	<	393.54
27	23.28	45.45	14.41	33.26	454.55	<	349.22
28	25.94	25.94	<	51.87	293.19	<	429.63
29	26.71	37.84	<	43.40	393.95	<	308.26
30	27.53	38.54	<	55.05	409.60	<	616.60
31	14.43	66.62	<	32.20	1724.41	<	278.70
32	17.66	77.26	<	52.98	960.26	<	392.94
33	n.a.	n.a.	n.a.	n.a.	n.a.	n.a.	n.a.
34	n.a.	n.a.	n.a.	n.a.	n.a.	n.a.	n.a.
35	n.a.	n.a.	n.a.	n.a.	n.a.	n.a.	n.a.
36	<	42.47	<	24.59	1015.87	<	139.70
37	34.81	18.49	25.02	50.03	174.03	<	312.16
38	28.57	41.75	<	21.98	468.08	<	408.75
39	24.98	66.26	<	40.19	569.19	<	278.08
A	30.62	48.12	<	27.34	507.49	<	323.74
B	34.15	38.55	12.12	53.98	499.01	17.63	358.01
C	25.48	38.77	<	15.51	363.35	<	386.62
D	53.55	59.02	<	15.30	859.02	63.39	228.42

< lower than detection limiet
n.a. not analysed

All expressed in parts per million (ppm)

ANNEX VIII: CALCULATION OF VARIOUS CORRELATIONS

Figure 5.1: Fe_2O_3 versus TiO_2

Samples: 32, 33, 34, 35 and 36
r^2 = 0.824
x-coefficient = -39.67
constant = 137.70

Samples: 32, 34, 35 and 36
r^2 = 0.986
x-coefficient = -40.95
constant = 142.23

Samples: 20, 21, 23, 24, 26, 27, 28, 29, 38, 39, A and B
r^2 = 0.821
x-coefficient = 173.82
constant = -228.27

Samples: 5, 6, 7, 8, 9, 10, 11, 12, 13, 14, 16, 17, 18, 19, 22, 25 and 37
r^2 = 0.645
x-coefficient = 31.37
constant = -20.95

Figure 5.2: Al_2O_3 versus TiO_2

Samples: 32, 33, 34, 35 and 36
r^2 = 0.822
x-coefficient = 14.68
constant = -9.82

Samples: 32, 34, 35 and 36
r^2 = 0.991
x-coefficient = 15.16
constant = -11.53

Samples: 20, 21, 23, 24, 26,27,28 and 29
r^2 = 0.75
x-coefficient = -37.10
constant = 80.68

Samples: 20, 21, 23, 24, 26, 27, 28, 29, 38, 39, A and B
r^2 = 0.68
x-coefficient = -65.51
constant = 120.25

Samples: 6, 8, 9, 10, 13, 14, 16, 17, 19, 22 and 25
r^2 = 0.413
x-coefficient = 22.80
constant = 2.76

Samples: 6, 8, 9, 10, 13, 14, 16, 17, 22 and 25
r^2 = 0.759
x-coefficient = 34.88
constant = -8.97

Samples: 5, 8, 11, 12, 18, 37 and C
r^2 = 0.818
x-coefficient = 8.75
constant = 12.25

Samples: 5, 8, 11, 18, 37 and C
r^2 = 0.985
x-coefficient = 10.63
constant = 10.53

ANNEX VIII: CALCULATION OF VARIOUS CORRELATIONS

Figure 5.3: SiO_2 versus TiO_2

Samples: 32, 33, 34, 35 and 36
r^2 = 0.775
x-coefficient = 24.96
constant = -29.24

Samples: 32, 34, 35 and 36
r^2 = 0.992
x-coefficient = 25.91
constant = -32.61

Samples: 20, 21, 23, 26, 27, 28, 29, 38, 39, A and B
r^2 = 0.831
x-coefficient = -98.55
constant = 191.62

Samples: 21, 21, 23, 24, 26, 27, 28, 29, 38, 39, A and B
r^2 = 0.845
x-coefficient = -105.51
constant = 202.09

Samples: 5, 6, 7, 8, 9, 10, 11, 12, 13, 14, 16, 17, 18, 19, 22, 25 and 37
r^2 = 0.523
x-coefficient = -28.53
constant = 93.78

Samples: 8, 9,1 0, 14, 16, 17, 18, 22, 25 and 37
r^2 = 0.710
x-coefficient = -63.79
constant = 127.45

Samples: 5, 6, 7, 11 and 12
r^2 = 0.742
x-coefficient = -17.65
constant = 81.90

Figure 5.4: SiO_2 versus Al_2O_3

Samples: 32, 33, 34, 35 and 36
r^2 = 0.980
x-coefficient = 0.57
constant = 7.92

Samples: 20, 21, 23, 26, 27, 28, 29 and 30
r^2 = 0.976
x-coefficient = 0.43
constant = 5.52

Samples: 20, 21, 23, 26, 27, 28, 29, 30, B, C and D
r^2 = 0.975
x-coefficient = 0.53
constant = 0.24

Samples: 8, 10, 13, 14, 16, 17, 18, 19, 20, 22, 24 and 25
r^2 = 0.979
x-coefficient = -0.63
constant = 65.94

ANNEX VIII: CALCULATION OF VARIOUS CORRELATIONS

Figure 5.5: Fe_2O_3 versus SiO_2

Samples: 32, 33, 34, 35 and 36
r^2 = 0.982
x-coefficient = -1.53
constant = 90.22

Samples: 23, 26, 27, 28, 29 and 30
r^2 = 0.992
x-coefficient = -1.46
constant = 94.45

Samples: 23, 26, 27, 28, 29, 30, 38, 39, A, B, C and D
r^2 = 0.963
x-coefficient = -1.69
constant = 106.20

Samples: 21, 23, 26, 27, 28, 29 and 30
r^2 = 0.997
x-coefficient = -1.50
constant = 96.18

Samples 8, 10, 13, 14, 16, 17, 18, 19, 20, 21, 22, 24
r^2 = 0.917
x-coefficient = -0.34
constant = 29.92

Samples: 5, 6, 7, 9, 11 and 12 and 25
r^2 = 0.712
x = -1.45
constant = 105.30

Figure 5.6: Fe_2O_3 versus Al_2O_3

Samples: 32, 33, 34, 35 and 36
r^2 = 0.989
x-coefficient = -2.68
constant = 110.78

Samples: 21, 23, 26, 27 28, 29 and 30
r^2 = 0.990
x-coefficient = -3.25
constant = 109.40

Samples: 21, 23, 26, 27, 28, 28, 29, 30, B, C and D
r^2 = 0.988
x-coefficient = -2.76
constant = 95.86

Samples: 8, 9, 10, 13, 14, 16, 17, 18, 19, 20, 21, 22, 24 and 25
r^2 = 0.743
x-coefficient = 0.49
constant = -4.38

Samples: 8, 10, 13, 14, 16, 17, 18, 19, 20, 21, 22, 24 and 25
r^2 = 0.879
x-coefficient = 0.51
constant = -5.07

PUBLICATIONS DEJA PARUES:
(SUITE DE LA PAGE INTERIEURE DU FRONTISPICE)

Publications de l'Antenne (suite)

13	A.H.M. Schutjes & W.F. van Driel	La classification locale des terres par les Mossi: paysans et pédologues parlent-ils le même langage ? Contribution au 1er Colloque International de l'AOCASS: Gestion Durable des Sols et de l'Environnement en Afrique Tropicale, Ouagadougou, 6 - 10 décembre 1994
14	H.B. Tammes, R.B. Kaboré & W.F. van Driel	L'effet de la matière organique sur la formation des croûtes et l'érosion des sols sableux au Burkina Faso. Contribution au 1er Colloque International de l'AOCASS: Gestion Durable des Sols et de l'Environnement en Afrique Tropicale, Ouagadougou, 6-10 décembre 1994
15	H.J.M Gijsbers J.J. Kessler M.K. Knevel	Dynamics and natural regeneration of woordy species in farmed parklands in the Sahel region (Province of Passore, Burkina Faso) In: Forest Ecology and Management 64 (1994) 1-12
16	J.J. Kessler	Usefulness of the human carrying capacity concept in assessing ecological sustainability of land-use in semi-arid regions. In Agriculture, Ecosystems & Environment 48 (1994) 273-284
17	J.J. Kessler P. Laban	Planning strategies and funding modalities for land rehabilitation. In: Land Degradation & Rehabilitation, Vol. 5, 25-32 (1994)
18	A. Blokland L. Stroosnijder	Sustainable agriculture and food security - a challenge to farmers, research and development in the Sahel. Chapter 4 from: Development-related research collaboration. A second look at the role of the Netherlands,C. Schweigman and I.A. van der Werf(eds), Royal Tropical Institute, Amsterdam, 1994
19	J. de Graaff L. Stroosnijder	L'évaluation économique des mesures CES au Sahel (présenté lors des 11ème Journées du Réseau Erosion "L'environnement humain de l'érosion, 20-22 septembre 1994, ORSTOM/E.N.S. St. CLOUD-Université PARIS VII)
20	E. H. van Haaften F.J.R. van de Vijver	Psychological consequences of environmental Degradation

Rapports des étudiants (violet)

1	M. Rietkerk	Les differences locales du sol et la capacité de régénération: une étude pour la régénération des écosystèmes sylvo-pastoraux Sahéliens, dans la Forêt Classée de Yabo (Burkina Faso)
2	S.J.T. Poutsma	Geografische Informatie Systemen en bodem- en waterconservering: een praktijkvoorbeeld
3	J. van Etten	Mesures de rendement dans les Bas-fonds de Damana, Kawara et Moadougou, rapport de stage
4	A. de Wit	L'effet du bilan hydrique sur la croissance des arbres tropicaux: une étude sur la distance optimale des diguettes à l'aide de quantité d'eau utilisée par l'Acacia Seyal
5	A. Florijn	Etude sur l'impact hydrologique des digues filtrantes sur l'humidité volumétrique du sol dans le bas-fond de Noh
6A	H.B. Tammes	Carte des états de surface du bassin versant de Solmiougou
6B	H.B. Tammes	L'effet de la matière organique des sols sableux de Burkina Faso sur la formation des croûtes et sur l'érosion
7	F. Kologo	Evaluation des techniques de restauration des sols dans les zones sylvo-pastorales de la province du Sanmatenga
8	A. Belemviré	Contribution à l'étude de la cartographie des états de surface et à l'estimation de la biomasse ligneuse aérienne à partir de l'image Landsat Thematic Mapper. Essais de Mesures radiométriques au sol. Etudes menées au Kaya
9	S. Idi	Evaluation des contraintes socio-économiques et techniques des plantations villageoises dans le Sanmatenga: étude de cas
11	M. de Haas	Assessment of aggregate stability of Sahelian soils from Burkina Faso
12	O. van Dam	Recherche du sol et de la télédétection à Kaya, Burkina Faso
13	J.C. den Boef	Les mesures de conversation des eaux et du sol dans trois villages de la province du Zoundwéogo.
14	P.A.J. Schaper	Les mesures de conservation des eaux et des sols dans trois villages de la province du Sanmatenga
15	A.R. Vriend	Un inventaire agro-socio-économique des ménages du plateau central du Burkina Faso
16	M.C. Minnaard	Une étude sociologique sur la coopération autour des mesures des conservations des eaux et des sols, dans un village Mossi, Burkina Faso.
19	T. Slaa	Contribution à la classification des espaces sylvo-pastoraux au niveau villageois dans le Sahel
21a	A. Bleumink	La goutte qui se fait déborder la surface: une recherche indicative à l'influence du climat local sur la dégradation des états de la surface
21b	A. Bleumink	La goutte qui se fait déborder la surface, supplément: les données obtenues de la station météo
23	K.O. Trouwborst	Soil moisture reserve development at soil-water conservation measures in Burkina Faso
24	I.H. Janssen	De invloed van korsten op afstroming en nutriëntenverliezen in de Sahel
26	L. Coolegem	Recherche des intensités de la pluie dans trois stations au Burkina Faso
27	L.A. Timmer	Une étude sur les buts et les types de taille du néré (Parkia biglobosa (Jacq.) Benth.) et la relation avec sa structure
29	A.T.A. Loozekoot	A plusieurs mains l'ouvrage avance! Une étude socio-économique de Barcé, Yakin et Salmintenga, trois villages dans la province de Zoundwéogo au sud de Burkina Faso
29a	A.T.A. Loozekoot	Land degradation, population pressure and agricultural intensification
30	J.D. Wijnhoud/A.J. Otto	Physical properties of soils in the Kaya area, Burkina Faso
31	C.M.J. Jans	Les occupations et les revenues des plusieurs ménages au Burkina Faso
32	E. Elkenbracht/A. ten Holte/ L. Otter/T.Slaa	Remote sensing and soil science of the Kaya area (Burkina Faso)

PUBLICATIONS DEJA PARUES (SUITE):

Rapports des étudiants (suite):

40	F. Elskamp	Les petits ruminants dans trois systèmes d'élevage dans la région de Manga, Burkina Faso.
44a	M. Kempkes	Analyse financière des cordons pierreux. Cas d'étude de Tagalla, province du Sanmatenga au Burkina Faso.
44b	M. Kempkes	Enquête socio-économique menée dans la provive du Sanmatenga au Burkina Faso durant la période sèche de 1994. Les résultats et leur analyse.
49	R. Geelhoed	Les pertes de nutriments dans le ruissellement et le sédiment et l'importance relative d'entraînement
50	S.I. Hillenaar	Infiltration characteristics of some selected sites in Zoundwéogo, Burkina Faso.
51	J. Suurmond	Rôle de l'élevage dans la zone traditionnelle de la province du Zoundwéogo.
58	A.A.C. Jellema	Faire une carte d'utilisation de la terre à l'aide de données-Landsat-TM, de photographies aeriènnes, et d'observations sur le terrain.
61a	M.Z. Steenis	Deriving sub-pixel soil characteristics in Northern Burkina Faso with spectral unmixing
64a	L. de Boer	Genesis of iron crusts in Burkina Faso.
64b	L. de Boer	Nutrient status of two water catchments in Burkina Faso.

AUTRES PUBLICATIONS

- Stroosnijder, L. et al. (1990). Bijdragen Saheldag LUW-KIT 1990: Aménagement du Terroir Villageois. LUW, Wageningen
- Kessler, J.J. et J. Boni (1991). L'Agroforesterie au Burkina Faso; Bilan et analyse de la situation actuelle. Tropical Resource Management Paper No. 1, Ministère de l'Environnement et du Tourisme et UAW, Wageningen, Pays-Bas
- Bognetteau-Verlinden, E., S van der Graaf et J.J. Kessler (1992). Aspects de l'aménagement intégré des ressources naturelles au Sahel. Tropical Resource Management Paper No. 2, SNV et AUW, Wageningen, Pays-Bas
- Vlaar, J.C.J. (Ed.), 1992. Les techniques de conservation des eaux et des sols dans les pays du Sahel. Rapport d'une étude effectuée dans le cadre de la collaboration entre le Comité Interafricain d'Etudes Hydrauliques (CIEH), Ouagadougou Burkina Faso, et l'Université Agronomique Wageningen (UAW), Wageningen, Pays Bas
- Graaff, J. de (1993). Soil Conservation and sustainable land use, an economic approach. Development Oriented Research in Agriculture no. 4, Royal Tropical Institute, Amsterdam, Pays-Bas
- Boer de, F. et J.J. Kessler (1993). Le système d'élevage Peulh dans le sud du Burkina Faso: une étude agro-écologique du département de Tô. Tropical Resource Management Paper No. 3, AUW, Wageningen, Pays-Bas
- Hoek van der, R. et al. (1994). Perspectives pour le développement soutenu des systèmes de production agrosylvopastorale au Sanmatenga, Burkina Faso. Tropical Resource Management Paper No. 4, AUW, Wageningen, Pays-Bas
- Briel van den, J. et al. (1994). L'aménagement des terroirs villageois: une contribution à la gestion durable des ressources naturelles. Etude de cas du projet Reboisement Rive Droite Téra, Niger. Tropical Resource Management Paper No. 5, AUW, Wageningen, Pays-Bas
- Kajembe, G.C. (1994). Indigenous management systems as a basis for community forestry in Tanzania: a case study of Dodoma urban and Lushoto Districts. Tropical Resource Management Papers No. 6, AUW, Wageningen, Pays Bas
- Hien, F.G. (1995). La régénération de l'espace sylvo-pastoral au Sahel: Une étude de mesures de conservation des eaux et des sols au Burkina Faso. Tropical Resource Management Papers No. 7, AUW, Wageningen, Pays-Bas.
- Zeeuw, F. de (1995). Sécurité foncière et gestion des ressources naturelles dans la Boucle du Mouhon - Burkina Faso. Tropical Resource Management Papers No. 9, AUW, Wageningen, Pays-Bas, 45 p.

– afwezig
(+) twijfelachtig
\+ 1 of 2 v/d sterkste lijnen
++ sterkere lijnen
+++ alleen sterkste lijnen ontbreken
++++ een goed detectie mogelijk

MONSTERS t.b.v. MICROMORFOLOGISCH ONDERZOEK.

Genomen door : Dick Legger
Ontvangen door : A. v. Dijk
Aantal : 34
Formaat : ~~groot~~/klein afdekken
Droge Impregnatie

Datum monstername : Sept. '92
Inleveringsdatum : 2-11-1992
Gewenste afleveringsdatum : 2.5.m.
In behandeling genomen : 2-11-1992
GeImpregneerd : 12-11-1992
Afgeleverd : 4-12-1992

Gegevens: Niger-Sahel. Project Hapex Sahel.
kaoliniet anataas hematiet goethiet

Nummer blikje	Monster-nummer	Horizont	Diepte	Nummer slijpplaat	Opmerkingen
1					Vallei FB
2	(+)	(+)	–	+++	Oase geel gerteente
3	++	+	–	–	Oase gebl. klei
4	–	–	–	–	Oase zand/steen Fe min.
5	+	+	++++	–	Oase gerteente Fe + Mn min.
6	(+)	(+)	–	calciet ++ –	Kaoliniet/gibbsiet
7	++	+	–	–	Gullie complex
8	–	–	++	++++	Plinthiet
9	–	–	–	++	Gele Plinthiet
10	+++	+	++	–	Terrasrest Rood
11	+++	++	–	–	Terrasrest wit
12	++	+		–	Gravell
13					3 g
14					2 g
15					4 g
16					5 g
17					gold 2 mix

PUBLICATIONS DEJA PARUES (SUITE):

Rapports des étudiants (suite):

40	F. Elskamp	Les petits ruminants dans trois systèmes d'élevage dans la région de Manga, Burkina Faso.
44a	M. Kempkes	Analyse financière des cordons pierreux. Cas d'étude de Tagalla, province du Sanmatenga au Burkina Faso.
44b	M. Kempkes	Enquête socio-économique menée dans la provive du Sanmatenga au Burkina Faso durant la période sèche de 1994. Les résultats et leur analyse.
49	R. Geelhoed	Les pertes de nutriments dans le ruissellement et le sédiment et l'importance relative d'entraînement
50	S.I. Hillenaar	Infiltration characteristics of some selected sites in Zoundwéogo, Burkina Faso.
51	J. Suurmond	Rôle de l'élevage dans la zone traditionnelle de la province du Zoundwéogo.
58	A.A.C. Jellema	Faire une carte d'utilisation de la terre à l'aide de données-Landsat-TM, de photographies aeriènnes, et d'observations sur le terrain.
61a	M.Z. Steenis	Deriving sub-pixel soil characteristics in Northern Burkina Faso with spectral unmixing
64a	L. de Boer	Genesis of iron crusts in Burkina Faso.
64b	L. de Boer	Nutrient status of two water catchments in Burkina Faso.

AUTRES PUBLICATIONS

- Stroosnijder, L. et al. (1990). Bijdragen Saheldag LUW-KIT 1990: Aménagement du Terroir Villageois. LUW, Wageningen
- Kessler, J.J. et J. Boni (1991). L'Agroforesterie au Burkina Faso; Bilan et analyse de la situation actuelle. Tropical Resource Management Paper No. 1, Ministère de l'Environnement et du Tourisme et UAW, Wageningen, Pays-Bas
- Bognetteau-Verlinden, E., S van der Graaf et J.J. Kessler (1992). Aspects de l'aménagement intégré des ressources naturelles au Sahel. Tropical Resource Management Paper No. 2, SNV et AUW, Wageningen, Pays-Bas
- Vlaar, J.C.J. (Ed.), 1992. Les techniques de conservation des eaux et des sols dans les pays du Sahel. Rapport d'une étude effectuée dans le cadre de la collaboration entre le Comité Interafricain d'Etudes Hydrauliques (CIEH), Ouagadougou Burkina Faso, et l'Université Agronomique Wageningen (UAW), Wageningen, Pays Bas
- Graaff, J. de (1993). Soil Conservation and sustainable land use, an economic approach. Development Oriented Research in Agriculture no. 4, Royal Tropical Institute, Amsterdam, Pays-Bas
- Boer de, F. et J.J. Kessler (1993). Le système d'élevage Peulh dans le sud du Burkina Faso: une étude agro-écologique du département de Tô. Tropical Resource Management Paper No. 3, AUW, Wageningen, Pays-Bas
- Hoek van der, R. et al. (1994). Perspectives pour le développement soutenu des systèmes de production agrosylvopastorale au Sanmatenga, Burkina Faso. Tropical Resource Management Paper No. 4, AUW, Wageningen, Pays-Bas
- Briel van den, J. et al. (1994). L'aménagement des terroirs villageois: une contribution à la gestion durable des ressources naturelles. Etude de cas du projet Reboisement Rive Droite Téra, Niger. Tropical Resource Management Paper No. 5, AUW, Wageningen, Pays-Bas
- Kajembe, G.C. (1994). Indigenous management systems as a basis for community forestry in Tanzania: a case study of Dodoma urban and Lushoto Districts. Tropical Resource Management Papers No. 6, AUW, Wageningen, Pays Bas
- Hien, F.G. (1995). La régénération de l'espace sylvo-pastoral au Sahel: Une étude de mesures de conservation des eaux et des sols au Burkina Faso. Tropical Resource Management Papers No. 7, AUW, Wageningen, Pays-Bas.
- Zeeuw, F. de (1995). Sécurité foncière et gestion des ressources naturelles dans la Boucle du Mouhon - Burkina Faso. Tropical Resource Management Papers No. 9, AUW, Wageningen, Pays-Bas, 45 p.

MONSTERS t.b.v. MICROMORFOLOGISCH ONDERZOEK.

Genomen door :

Ontvangen door :

Aantal : Formaat : ~~groot~~/klein

Datum monstername :

Inleveringsdatum :

Gewenste afleveringsdatum :

In behandeling genomen :

Geïmpregneerd :

Afgeleverd :

monster 24 t/m 34 Richting.

Gegevens:

Nummer blikje	Monster-nummer	Horizont	Diepte	Nummer slijpplaat	Opmerkingen
18					File 15
19					File 10
20					78
21					File 12
22					LR
23					LE
24					K 19
25					38
26					K 22
27					K 26 4 lagen korst
28					r 2
29					k 2
30					r 4
31					r 8 3 lagen korst
32					k 8 2 lagen korst
33					k 20 2 lagen korst
34					k 30 4 lagen korst

Richting

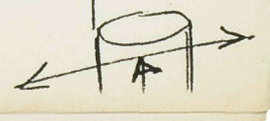

PUBLICATIONS DEJA PARUES (SUITE):

Rapports des étudiants (suite):

40	F. Elskamp	Les petits ruminants dans trois systèmes d'élevage dans la région de Manga, Burkina Faso.
44a	M. Kempkes	Analyse financière des cordons pierreux. Cas d'étude de Tagalla, province du Sanmatenga au Burkina Faso.
44b	M. Kempkes	Enquête socio-économique menée dans la provive du Sanmatenga au Burkina Faso durant la période sèche de 1994. Les résultats et leur analyse.
49	R. Geelhoed	Les pertes de nutriments dans le ruissellement et le sédiment et l'importance relative d'entraînement
50	S.I. Hillenaar	Infiltration characteristics of some selected sites in Zoundwéogo, Burkina Faso.
51	J. Suurmond	Rôle de l'élevage dans la zone traditionnelle de la province du Zoundwéogo.
58	A.A.C. Jellema	Faire une carte d'utilisation de la terre à l'aide de données-Landsat-TM, de photographies aeriènnes, et d'observations sur le terrain.
61a	M.Z. Steenis	Deriving sub-pixel soil characteristics in Northern Burkina Faso with spectral unmixing
64a	L. de Boer	*Genesis of iron crusts in Burkina Faso.*
64b	L. de Boer	Nutrient status of two water catchments in Burkina Faso.

AUTRES PUBLICATIONS

- Stroosnijder, L. et al. (1990). Bijdragen Saheldag LUW-KIT 1990: Aménagement du Terroir Villageois. LUW, Wageningen
- Kessler, J.J. et J. Boni (1991). L'Agroforesterie au Burkina Faso; Bilan et analyse de la situation actuelle. Tropical Resource Management Paper No. 1, Ministère de l'Environnement et du Tourisme et UAW, Wageningen, Pays-Bas
- Bognetteau-Verlinden, E., S van der Graaf et J.J. Kessler (1992). Aspects de l'aménagement intégré des ressources naturelles au Sahel. Tropical Resource Management Paper No. 2, SNV et AUW, Wageningen, Pays-Bas
- Vlaar, J.C.J. (Ed.), 1992. Les techniques de conservation des eaux et des sols dans les pays du Sahel. Rapport d'une étude effectuée dans le cadre de la collaboration entre le Comité Interafricain d'Etudes Hydrauliques (CIEH), Ouagadougou Burkina Faso, et l'Université Agronomique Wageningen (UAW), Wageningen, Pays Bas
- Graaff, J. de (1993). Soil Conservation and sustainable land use, an economic approach. Development Oriented Research in Agriculture no. 4, Royal Tropical Institute, Amsterdam, Pays-Bas
- Boer de, F. et J.J. Kessler (1993). Le système d'élevage Peulh dans le sud du Burkina Faso: une étude agro-écologique du département de Tô. Tropical Resource Management Paper No. 3, AUW, Wageningen, Pays-Bas
- Hoek van der, R. et al. (1994). Perspectives pour le développement soutenu des systèmes de production agrosylvopastorale au Sanmatenga, Burkina Faso. Tropical Resource Management Paper No. 4, AUW, Wageningen, Pays-Bas
- Briel van den, J. et al. (1994). L'aménagement des terroirs villageois: une contribution à la gestion durable des ressources naturelles. Etude de cas du projet Reboisement Rive Droite Téra, Niger. Tropical Resource Management Paper No. 5, AUW, Wageningen, Pays-Bas
- Kajembe, G.C. (1994). Indigenous management systems as a basis for community forestry in Tanzania: a case study of Dodoma urban and Lushoto Districts. Tropical Resource Management Papers No. 6, AUW, Wageningen, Pays Bas
- Hien, F.G. (1995). La régénération de l'espace sylvo-pastoral au Sahel: Une étude de mesures de conservation des eaux et des sols au Burkina Faso. Tropical Resource Management Papers No. 7, AUW, Wageningen, Pays-Bas.
- Zeeuw, F. de (1995). Sécurité foncière et gestion des ressources naturelles dans la Boucle du Mouhon - Burkina Faso. Tropical Resource Management Papers No. 9, AUW, Wageningen, Pays-Bas, 45 p.

Datum: 07-10-92
Onderwerp: aanvraag voor impregnatie
Gebied: Niger-Sahel
Project: Hapex Sahel
Aanvrager: D. Legger.

Gaarne de volgende monsters inpregneren voor micromorfologisch onderzoek.
Het gaat doel is:

-na te gaan of het moedermatriaal op diverse plekken in het karteringsgebied in Niger gelijk is en waaruit dat matriaal dan bestaat (Monsters 1-11)
-de locatie van het vrije ijzer te bepalen. De uitkomst hiervan zal gebruikt worden voor correlaties met reeds bepaalde di-electrische waarden (monsters 12- 20);
-het bestuderen van verschillende soorten korsten om een indruk te krijgen van hun ontstaan (monsters 21-31)

1: In vallei bij FB, vlakbij market
2: Bij oase, geel gesteente
3: ,, ,, , gebleekte klei
4: ,, ,, , zand steen met kleine Fe mineralen
5: Bij oase, getseente met grote Fe en Mn mineralen
6: Kaoliniet/gibbsiet achtige dagzoming bij N-plateau,poppetjes
7: In gulliecomplex tussen N plateau en punt 6
8: Verhard plinthiet op plateau
9: Geler verhard plinthiet op plateau
10: Terrasrest langs weg bij hut A, rood
11: ,, ,, ,, ,, ,, ,, A, wit

12:	gravel1	gravel D-site
13:	3g	centrum open plek Z van zuidplateau
14:	2g	rand ,, ,, ,, ,, ,,
15:	4g	open plek in tigerbush bij monster 12
16:	5g	op piedmont van zuidplareau (transect peter 2)
17:	gold2 mix	degr. bush, men monster
18:	file 15	duin 1-6 oranje-bruin zand rand helling duin Z van FB
19:	file 10	duin 1-1 bij monster 19
20:	7g	wit zand bij markt FB (transect)
21:	file 12	zuiden FB wit zand uit dal
22:	LR	klei met veel Fe
23:	LE	klei met veel Fe
24:	k19	pied 1-5 rode kleikorst piedmont Z plateau
25:	3g	centrum open plek Z van Z-plateau
26:	k22	pied 1-17 bruine korst met zand piedmont Z plateau
27:	k26	korst met o.m. bij FB, file uit refl. metingen
28:	r2	korst onderaan s woongebied bij degraded b.g., van hydro
29:	k2	rode korst met klei in groene plek spotbeeld bij A
30:	r4	TER korst van FB
31:	r8	krul korst in tiger bush
32:	k8	niet te lezen
33:	k20	pied 1-4 groen algkorst met rood en bruin piedmont Z plat.
34:	k30	krulkorst op plateau tiger bush

Dick Legger

PUBLICATIONS DEJA PARUES (SUITE):

Rapports des étudiants (suite):

40	F. Elskamp	Les petits ruminants dans trois systèmes d'élevage dans la région de Manga, Burkina Faso.
44a	M. Kempkes	Analyse financière des cordons pierreux. Cas d'étude de Tagalla, province du Sanmatenga au Burkina Faso.
44b	M. Kempkes	Enquête socio-économique menée dans la provive du Sanmatenga au Burkina Faso durant la période sèche de 1994. Les résultats et leur analyse.
49	R. Geelhoed	Les pertes de nutriments dans le ruissellement et le sédiment et l'importance relative d'entraînement
50	S.I. Hillenaar	Infiltration characteristics of some selected sites in Zoundwéogo, Burkina Faso.
51	J. Suurmond	Rôle de l'élevage dans la zone traditionnelle de la province du Zoundwéogo.
58	A.A.C. Jellema	Faire une carte d'utilisation de la terre à l'aide de données-Landsat-TM, de photographies aeriènnes, et d'observations sur le terrain.
61a	M.Z. Steenis	Deriving sub-pixel soil characteristics in Northern Burkina Faso with spectral unmixing
64a	L. de Boer	Genesis of iron crusts in Burkina Faso.
64b	L. de Boer	Nutrient status of two water catchments in Burkina Faso.

AUTRES PUBLICATIONS

- Stroosnijder, L. et al. (1990). Bijdragen Saheldag LUW-KIT 1990: Aménagement du Terroir Villageois. LUW, Wageningen
- Kessler, J.J. et J. Boni (1991). L'Agroforesterie au Burkina Faso; Bilan et analyse de la situation actuelle. Tropical Resource Management Paper No. 1, Ministère de l'Environnement et du Tourisme et UAW, Wageningen, Pays-Bas
- Bognetteau-Verlinden, E., S van der Graaf et J.J. Kessler (1992). Aspects de l'aménagement intégré des ressources naturelles au Sahel. Tropical Resource Management Paper No. 2, SNV et AUW, Wageningen, Pays-Bas
- Vlaar, J.C.J. (Ed.), 1992. Les techniques de conservation des eaux et des sols dans les pays du Sahel. Rapport d'une étude effectuée dans le cadre de la collaboration entre le Comité Interafricain d'Etudes Hydrauliques (CIEH), Ouagadougou Burkina Faso, et l'Université Agronomique Wageningen (UAW), Wageningen, Pays Bas
- Graaff, J. de (1993). Soil Conservation and sustainable land use, an economic approach. Development Oriented Research in Agriculture no. 4, Royal Tropical Institute, Amsterdam, Pays-Bas
- Boer de, F. et J.J. Kessler (1993). Le système d'élevage Peulh dans le sud du Burkina Faso: une étude agro-écologique du département de Tô. Tropical Resource Management Paper No. 3, AUW, Wageningen, Pays-Bas
- Hoek van der, R. et al. (1994). Perspectives pour le développement soutenu des systèmes de production agrosylvopastorale au Sanmatenga, Burkina Faso. Tropical Resource Management Paper No. 4, AUW, Wageningen, Pays-Bas
- Briel van den, J. et al. (1994). L'aménagement des terroirs villageois: une contribution à la gestion durable des ressources naturelles. Etude de cas du projet Reboisement Rive Droite Téra, Niger. Tropical Resource Management Paper No. 5, AUW, Wageningen, Pays-Bas
- Kajembe, G.C. (1994). Indigenous management systems as a basis for community forestry in Tanzania: a case study of Dodoma urban and Lushoto Districts. Tropical Resource Management Papers No. 6, AUW, Wageningen, Pays Bas
- Hien, F.G. (1995). La régénération de l'espace sylvo-pastoral au Sahel: Une étude de mesures de conservation des eaux et des sols au Burkina Faso. Tropical Resource Management Papers No. 7, AUW, Wageningen, Pays-Bas.
- Zeeuw, F. de (1995). Sécurité foncière et gestion des ressources naturelles dans la Boucle du Mouhon - Burkina Faso. Tropical Resource Management Papers No. 9, AUW, Wageningen, Pays-Bas, 45 p.

Dick Legger. Niger-Sahel Project Hapex Sahel

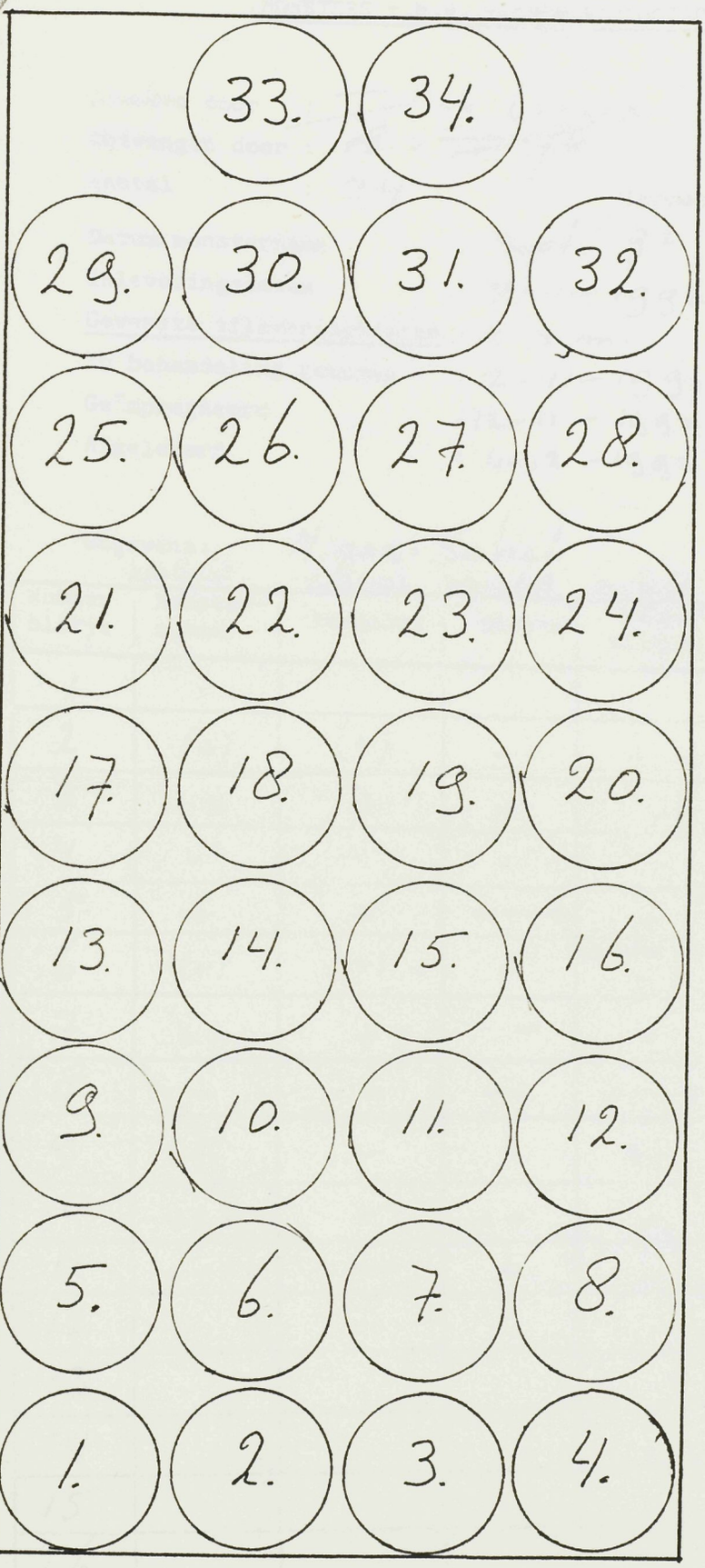

VOOR (situatie container)

Monster 24 t/m 34

Richting

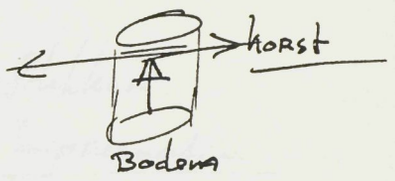

monster 27 4 lagen horst
monster 31 3 lagen horst
monster 32 2 lagen horst
monster 33 2 lagen horst
monster 34 4 lagen horst.

Karton tussen de lagen